NASA TM X-815



# TECHNICAL MEMORANDUM

X-815

## AERODYNAMIC CHARACTERISTICS AT MACH NUMBERS OF 2.30, 2.60, AND 2.96 OF A SUPERSONIC TRANSPORT MODEL WITH A BLENDED WING-BODY, VARIABLE-SWEEP AUXILIARY WING PANELS, OUTBOARD TAIL SURFACES, AND A DESIGN MACH NUMBER OF 2.6

By A. Warner Robins, M. Leroy Spearman, and Roy V. Harris, Jr.

Langley Research Center
Langley Station, Hampton, Va.

NATIONAL AERONAUTICS AND SPACE ADMINISTRATION

WASHINGTON

April 1963

NATIONAL AERONAUTICS AND SPACE ADMINISTRATION

TECHNICAL MEMORANDUM X-815

# AERODYNAMIC CHARACTERISTICS AT MACH NUMBERS OF 2.30, 2.60, AND 2.96 OF A SUPERSONIC TRANSPORT MODEL WITH A BLENDED WING-BODY, VARIABLE-SWEEP AUXILIARY WING PANELS, OUTBOARD TAIL SURFACES, AND A DESIGN MACH NUMBER OF 2.6

By A. Warner Robins, M. Leroy Spearman,
and Roy V. Harris, Jr.

## ABSTRACT

The investigation was conducted in the Langley Unitary Plan wind tunnel and includes the longitudinal and lateral aerodynamic characteristics for angles of attack up to about 10°. Tests were made with various combinations of component parts and with various deflections of the pitch control for the configuration with the retracted wing.

NATIONAL AERONAUTICS AND SPACE ADMINISTRATION

TECHNICAL MEMORANDUM X-815

# AERODYNAMIC CHARACTERISTICS AT MACH NUMBERS OF 2.30, 2.60, AND 2.96 OF A SUPERSONIC TRANSPORT MODEL WITH A BLENDED WING-BODY, VARIABLE-SWEEP AUXILIARY WING PANELS, OUTBOARD TAIL SURFACES, AND A DESIGN MACH NUMBER OF 2.6*

By A. Warner Robins, M. Leroy Spearman,
and Roy V. Harris, Jr.

## SUMMARY

An investigation has been made in the Langley Unitary Plan wind tunnel at Mach numbers of 2.30, 2.60, and 2.96 to determine the longitudinal and lateral aerodynamic characteristics of a model of a variable-sweep supersonic transport configuration with a design Mach number of 2.6 (SCAT 15-2.6). The configuration had a highly swept wing with horizontal and vertical tails attached to the wing tips and four engine nacelles attached to the underside of the wing.

The results indicated a significant improvement in performance over previously tested versions of the configuration in that the maximum trimmed values of lift-drag ratio obtained varied from about 7 at a Mach number of 2.30 to about 6.5 at a Mach number of 2.96. The trimmed lift-drag ratios varied only slightly over a fairly large range of stability level and the maximum value of trimmed lift-drag ratio at each Mach number occurred for a static margin of about 15 percent mean aerodynamic chord. Positive directional stability and a positive effective dihedral were indicated for the angle-of-attack range required for cruising flight.

## INTRODUCTION

The attainment of a commercially acceptable long-range supersonic transport aircraft will require higher levels of performance throughout the speed range than those normally associated with military aircraft designs. The National Aeronautics and Space Administration has had an intensive research program underway to provide the research background necessary to define and meet the transport design requirements. Conceptual configuration studies have been made to apply

[redacted]

the research results to configurations which may meet these requirements. The present concept (SCAT 15-2.6) has a highly swept wing blended with the fuselage. Vertical tails are located at the wing tips and the horizontal tail surfaces are located outboard of the vertical surfaces. Four nacelles are mounted below the wing to simulate engine installations. The configuration is equipped with variable-sweep auxiliary wing panels that can be fully retracted to form a part of the basic swept wing for high-speed flight or can be swept forward to increase the aerodynamic efficiency for low-speed flight.

In order to facilitate an early determination of the aerodynamic characteristics of the concept throughout the speed range, a model which did not incorporate wing camber and twist was tested and the results are contained in references 1 and 2. Another version of the model having a cambered body and a cambered and twisted wing optimized for a Mach number of 2.2 was investigated and the results are presented in reference 3. An additional version of the configuration having a wing twist and camber and a design Mach number of 2.6 was investigated, and the results obtained at supersonic speeds are presented herein for the configuration with the auxiliary wing panels fully retracted.

## COEFFICIENTS AND SYMBOLS

The results are referred to the body-axis system except the lift and drag coefficients which are referred to the stability-axis system. The moment reference point is at a longitudinal station corresponding to 75.9 percent of the body length.

The coefficients and symbols are defined as follows:

$b$ reference wing span excluding horizontal tail, 16.00 in.

$C_D$ drag coefficient, Drag/qS

$C_{D,o}$ zero-lift drag coefficient

$C_L$ lift coefficient, Lift/qS

$C_{L_\alpha}$ lift-curve slope

$C_l$ rolling-moment coefficient, Rolling moment/qSb

$C_m$ pitching-moment coefficient, Pitching moment/qS$\bar{c}$

$C_n$ yawing-moment coefficient, Yawing moment/qSb

$C_Y$ side-force coefficient, Side force/qS

$c$ local chord

| | |
|---|---|
| $\bar{c}$ | mean aerodynamic chord of reference wing, 15.66 in. |
| L/D | lift-drag ratio |
| M | free-stream Mach number |
| q | free-stream dynamic pressure, lb/sq in. |
| R | Reynolds number based on $\bar{c}$ |
| S | reference wing area including fuselage intercept but excluding horizontal tail, 219.464 sq in. |
| t | local thickness |
| $\alpha$ | angle of attack, deg |
| $\beta$ | angle of sideslip, deg |
| $\delta_h$ | horizontal-tail deflection, deg |
| $C_{l_\beta}$ | effective-dihedral parameter, $\partial C_l/\partial\beta$ at $\beta = 0^\circ$ |
| $C_{n_\beta}$ | directional-stability parameter, $\partial C_n/\partial\beta$ at $\beta = 0^\circ$ |
| $C_{Y_\beta}$ | side-force parameter, $\partial C_Y/\partial\beta$ at $\beta = 0^\circ$ |
| $\frac{\partial C_m}{\partial C_L}$ | longitudinal-stability parameter (or static margin, percent $\bar{c}$) |

Subscripts:

| | |
|---|---|
| max | maximum |
| min | minimum |

Model component designations:

| | |
|---|---|
| B | body |
| E | engine nacelle |
| H | horizontal tail |
| V | vertical tail |
| W | wing |

## MODEL AND APPARATUS

Details of the model are shown in figures 1 and 2 and the geometric characteristics are presented in table I. The normal area distributions for the model are presented in table II. The model was constructed so that various combinations of component parts could be investigated. The model was not equipped with a movable auxiliary wing panel but represented the configuration with the variable-sweep auxiliary wing panels fixed and smoothly faired in the fully retracted position. The horizontal tail surfaces could be adjusted to various deflection angles.

The model was mounted in the tunnel on a remote-controlled sting, and force measurements were made through the use of a six-component internal strain-gage balance.

## TESTS AND CORRECTIONS

For all tests, the Reynolds number based on $\bar{c}$ was $3.71 \times 10^6$ and the stagnation temperature was 150° F. The stagnation dewpoint was maintained sufficiently low to prevent condensation effects in the test section. Other test conditions are as follows:

| Mach number | Stagnation pressure, lb/sq ft |
|---|---|
| 2.30 | 2,170 |
| 2.60 | 2,537 |
| 2.96 | 3,073 |

Tests were made through an angle-of-attack range of about -4° to 10° and through a sideslip range of about -4° to 6°. The angles of attack and sideslip were corrected for the deflection of the balance and sting under load. The balance-chamber and base pressures were measured, and the drag force was adjusted to a base pressure equal to free-stream static pressure. In addition the drag results have been corrected for the internal skin-friction drag of the ducts as well as for the drag component of the normal force produced by the air which passes through the nacelles.

In order to assure a turbulent boundary layer, transition strips of No. 60 carborundum grit were applied near the nose of the body and near the leading edges of the wing and tails. Transition strips were located near the inlets on both the outer and inner surfaces of the engine nacelles with No. 80 grit on the outer surface and No. 120 grit on the inner surface. The minimum drag level for the complete configuration at $M = 2.96$ was measured over a Reynolds number range from $1.82 \times 10^6$ to $6.52 \times 10^6$ and the results (fig. 3) indicate good

agreement between the experimental measurements and theoretical turbulent skin-friction variation for Reynolds number above about $3.3 \times 10^6$.

## PRESENTATION OF RESULTS

The results of the investigation are presented in the following figures:



## DISCUSSION

### Longitudinal Aerodynamic Characteristics

The longitudinal aerodynamic characteristics for various combinations of model components are presented in figure 4. The pitching-moment variations for the basic wing-body indicate a marked tendency toward longitudinal instability with increasing lift primarily because of the inherent instability of the body. This characteristic of the body is especially pronounced because of the exceptionally far rearward location of the moment center. The addition of the engines provides a stabilizing increment in pitching moment that increases with increasing lift so that the high-lift instability is considerably lessened. This effect results from the influence of the pressure field induced by the engine nacelles on the lower surface of the wing. These pressures produce a positive increment of lift aft of the moment center which increases with increasing angle of attack because of the increase in local dynamic pressure beneath the wing. The addition of the horizontal tails provides an increase in lift-curve slope and a further increase in stability so that the tendency toward instability for the complete configuration is considerably reduced and, in any case, is confined to lift coefficients considerably above that for maximum L/D.

The twist and camber distribution of the basic wing-body combination is such that a substantial increment of lift is obtained at $\alpha = 0^\circ$ and a substantial increment of $C_m$ is obtained at zero lift. Although the presence of the engine nacelles tends to reduce the pitching moment at zero lift, the complete configuration still displays significant self-trimming characteristics.

The drag results indicate that the vertical tails, because they are small, have no measurable effect on either the minimum drag or the drag due to lift.

The addition of the horizontal tails, however, does produce an increase in minimum drag but a decrease in drag due to lift so that the maximum values of L/D are increased by the presence of the horizontal tails. The addition of the engine nacelles also causes an increase in minimum drag but a decrease in drag due to lift so that only a slight decrease in the maximum values of L/D occurs. The decrease in drag due to lift provided by the engines is caused, in part, by the favorable interference lift of the engines and, in part, by the cant angle of the nacelles that is intended to provide a minimum increment of drag near cruise lift.

The longitudinal parameters for the complete model are summarized and compared with the parameters for previous versions of the Scat 15 configuration in figure 5. Of particular significance is the progressive improvement in performance for the configuration concept as indicated by the increased level of $(L/D)_{max}$.

## Longitudinal Control

Deflection of the horizontal tails (fig. 6) provides a linear variation of pitch control effectiveness that is essentially constant throughout the lift range. Because of the inherent positive values of $C_m$ at zero lift, it is possible to provide stable trim points for the configuration even with positive control deflections. Deflecting the tails from 2° to -2° generally produces an improvement in drag due to lift and an increase in $(L/D)_{max}$. Note that a tail deflection of -2° more nearly alines the horizontal tails with the tip chord of the wing. A deflection of -6° results in only a slight reduction in $(L/D)_{max}$.

The data presented in figure 6 have been used to determine the maximum trimmed values of L/D for various levels of longitudinal stability and these results are presented in figure 7. The results indicate little change in trimmed L/D over a fairly large range of stability because of the combined effects of large positive values of $C_m$ at zero lift and the beneficial effects of upwash at the tails. Similar results have been obtained for other configurations having outboard tails. (See ref. 4, for example.) The maximum values of L/D occur for a stability level of about -0.15, and decreasing the static margin to lower values results in a slight decrease in L/D since positive deflections of the tails are then required for trimming. The maximum trimmed values of L/D obtained for a static margin of 15 percent $\bar{c}$ vary from about 7 at $M = 2.30$ to about 6.5 at $M = 2.96$.

## Lateral Aerodynamic Characteristics

The basic sideslip data presented in figure 8, for angles of attack near that required for $(L/D)_{max}$, indicate generally linear variations up to sideslip angles of at least 4°. The variations of the sideslip derivatives with angle of attack are presented in figure 9. The results indicate that, for each Mach number, the complete model maintains a reasonably high level of directional stability to angles of attack well above that for optimum cruising flight. The

decrease in $C_{n_\beta}$ that occurs with increasing angle of attack is caused primarily by the wing-body combination for which an increasing instability would be expected as a result of the large amount of the body forward of the moment center. The addition of the engines provides a stabilizing increment of $C_{n_\beta}$ that tends to increase with increasing $\alpha$ because of the increase in local dynamic pressure on the underside of the wing. In the lower angle-of-attack range, the addition of the engines alone is sufficient to provide a slight amount of positive directional stability. The addition of the tails provides a significant increment of $C_{n_\beta}$ in view of the relatively small size of the vertical tails and this increment decreases only slightly with increasing angle of attack. The separate increments of $C_{n_\beta}$ due to the engines and the vertical tails are directly additive in producing the $C_{n_\beta}$ level for the complete configuration.

The variation of $C_{l_\beta}$ with $\alpha$ is reasonably linear and indicates a positive dihedral effect for all configurations. In a manner similar to that for other SCAT 15 models (refs. 2 and 3), the effect of both the vertical tails and the nacelles is to increase the positive dihedral effect $\left(-C_{l_\beta}\right)$. The increase associated with the tails is due to the fact that the major portion of the tail area is above the roll axis; whereas, the increase associated with the nacelles is due to a lift interference effect induced by the engines.

## CONCLUDING REMARKS

An investigation has been made in the Langley Unitary Plan wind tunnel at Mach numbers of 2.30, 2.60, and 2.96 to determine the longitudinal and lateral aerodynamic characteristics of a model of a variable-sweep supersonic transport configuration with a design Mach number of 2.6 (SCAT 15-2.6). The configuration had a highly swept wing with horizontal and vertical tails attached to the wing tips and four engine nacelles attached to the underside of the wing.

The results indicated a significant improvement in performance over previously tested versions of the configuration in that the maximum trimmed values of lift-drag ratio obtained varied from about 7 at a Mach number of 2.30 to about 6.5 at a Mach number of 2.96. The trimmed lift-drag ratios varied only slightly over a fairly large range of stability level, and the maximum value of trimmed lift-drag ratio at each Mach number occurred for a static margin of about 15 percent mean aerodynamic chord. The configuration indicated positive directional stability and a positive effective dihedral for the angle-of-attack range required for cruising flight.

Langley Research Center,
National Aeronautics and Space Administration,
Langley Station, Hampton, Va., March 1, 1963.

## REFERENCES


1. Alford, William J., Jr., Hammond, Alexander D., and Henderson, William P.: Low-Speed Stability Characteristics of a Supersonic Transport Model With a Blended Wing-Body, Variable-Sweep Auxiliary Wing Panels, Outboard Tail Surfaces, and Simplified High-Lift Devices. NASA TM X-802, 1963.

2. Spearman, M. Leroy, Driver, Cornelius, and Robins, A. Warner: Aerodynamic Characteristics at Mach Numbers of 2.30, 2.96, and 3.50 of a Supersonic Transport Model With a Blended Wing-Body, Variable-Sweep Auxiliary Wing Panels, and Outboard Tail Surfaces. NASA TM X-803, 1963.

3. Driver, Cornelius, Spearman, M. Leroy, and Corlett, William A.: Aerodynamic Characteristics at Mach Numbers From 1.61 to 2.86 of a Supersonic Transport Model With a Blended Wing-Body, Variable-Sweep Auxiliary Wing Panels, Outboard Tail Surfaces, and a Design Mach Number of 2.2. NASA TM X-817, 1963.

4. Driver, Cornelius, and Spearman, M. Leroy: Static Stability and Control Characteristics of an Airplane Model With Tail Surfaces Outboard of the Wing Tips at a Mach Number of 2.01. NASA TM X-47, 1959.

TABLE I.- GEOMETRIC CHARACTERISTICS OF THE MODEL

| | |
|---|---|
| Wing: | |
| Sweep angle of leading edge, deg | 75 |
| Sweep angle of trailing edge, deg | 56.18 |
| Aspect ratio | 1.166 |
| Span (reference wing), in. | 16.0 |
| Area (reference wing), sq in. | 219.464 |
| Root chord, in. | 22.674 |
| Tip chord (including auxiliary wing panel), in. | 4.759 |
| Mean aerodynamic chord, in. | 15.666 |
| Fuselage: | |
| Length, in. | 40.842 |
| Balance-chamber area, sq in. | 2.680 |
| Horizontal tail: | |
| Area (both), sq in. | 16.570 |
| Airfoil section | Circular arc (t/c = 0.03) |
| Vertical tail: | |
| Area (both), sq in. | 16.124 |
| Airfoil section | Half circular arc (t/c = 0.02) |
| Nacelles: | |
| Length, in. | 7.500 |
| Capture area (each), sq in. | 0.704 |
| Base area (each), sq in. | 0.749 |
| Inboard nacelle: | |
| Cant angle | 0°45' |
| Longitudinal distance from nose of model to lip of nacelle, in. | 32.6 |
| Lateral distance from center line of model to center line of nacelle, in. | 2.500 |
| Vertical distance from model reference line to nacelle center line, in. | 0.937 |
| Outboard nacelle: | |
| Cant angle | 1°30' |
| Longitudinal distance from nose of model to lip of nacelle, in. | 38.1 |
| Lateral distance from center line of model to center line of nacelle, in. | 5.000 |
| Vertical distance from model reference line to nacelle center line, in. | 0.462 |
| Wetted area ratio | 3.531 |
| $\frac{(\text{Volume})^{2/3}}{\text{Reference area}}$ | 0.175 |

TABLE II.- AREA DISTRIBUTION OF COMPLETE MODEL

| Longitudinal station, in. | Cross-sectional area, sq in. | Longitudinal station, in. | Cross-sectional area, sq in. |
|---|---|---|---|
| 0 | 0 | 26.017 | 7.336 |
| 1.001 | .063 | 27.017 | 7.690 |
| 2.001 | .201 | 28.018 | 7.998 |
| 3.002 | .419 | 29.019 | 8.271 |
| 4.003 | .700 | 30.019 | 8.442 |
| 5.003 | 1.034 | | |
| | | 31.020 | 8.548 |
| 6.004 | 1.399 | 32.020 | 8.588 |
| 7.004 | 1.779 | 33.021 | 8.724 |
| 8.005 | 2.191 | 34.022 | 9.098 |
| 9.006 | 2.665 | 35.022 | 9.018 |
| 10.006 | 3.135 | | |
| | | 36.023 | 8.814 |
| 11.007 | 3.546 | 37.024 | 8.285 |
| 12.008 | 3.917 | 38.024 | 7.477 |
| 13.008 | 4.272 | 39.025 | 6.942 |
| 14.009 | 4.595 | 40.026 | 6.686 |
| 15.010 | 4.876 | | |
| | | 41.026 | 6.452 |
| 16.010 | 5.125 | 42.027 | 6.503 |
| 17.011 | 5.294 | 43.028 | 6.219 |
| 18.012 | 5.366 | 44.028 | 6.040 |
| 19.012 | 5.437 | 45.029 | 6.279 |
| 20.013 | 5.540 | | |
| | | 46.029 | 6.591 |
| 21.013 | 5.699 | 47.030 | 6.501 |
| 22.014 | 5.916 | 48.031 | 6.052 |
| 23.015 | 6.226 | 49.031 | 5.653 |
| 24.015 | 6.581 | 50.032 | 5.480 |
| 25.016 | 6.959 | | |

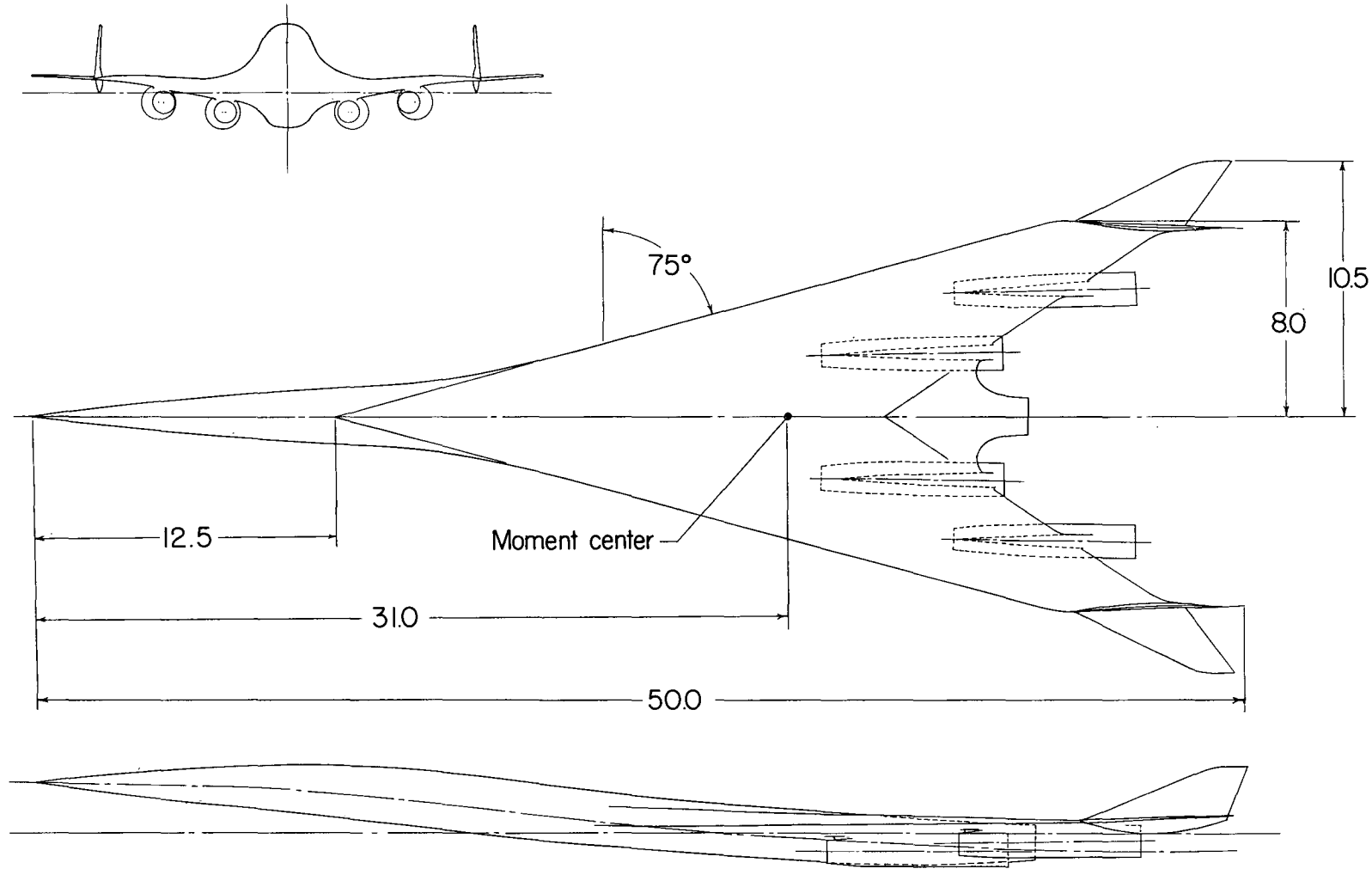


(a) Complete configuration.

Figure 1.- Details of model. All linear dimensions are in inches.

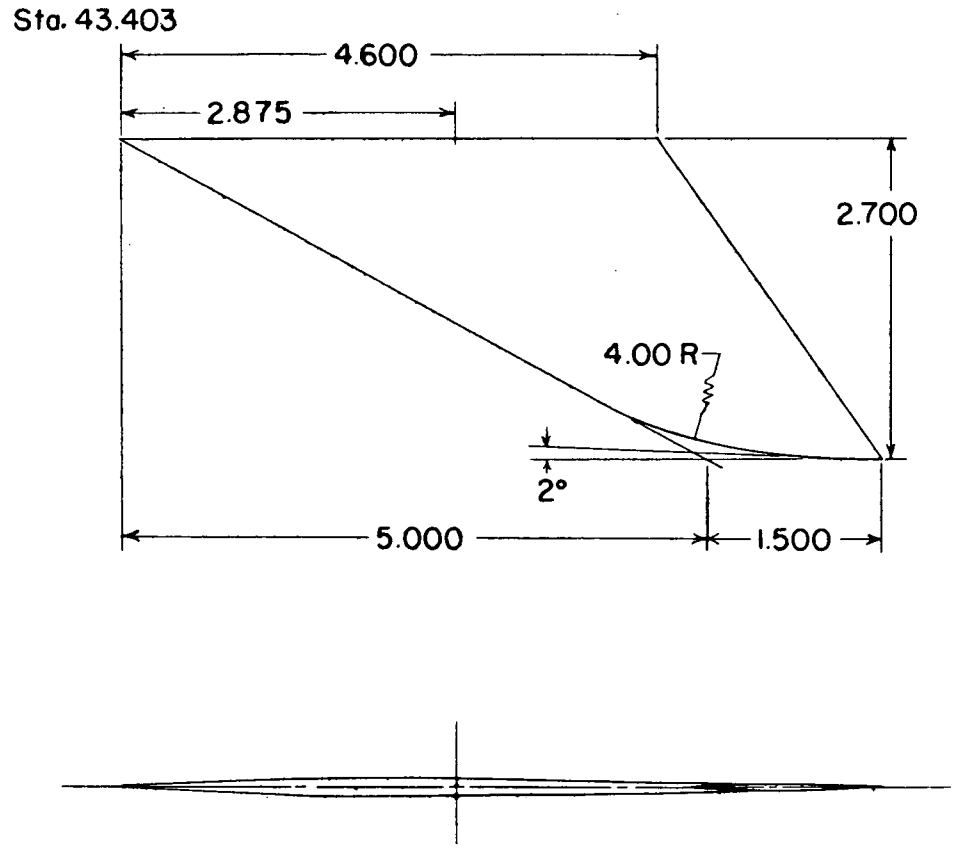


(b) Details of horizontal tail.

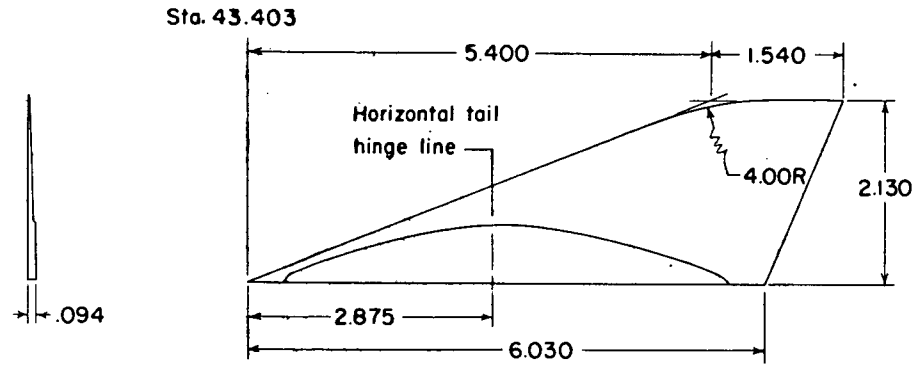


(c) Details of vertical tail.

Figure 1.- Continued.

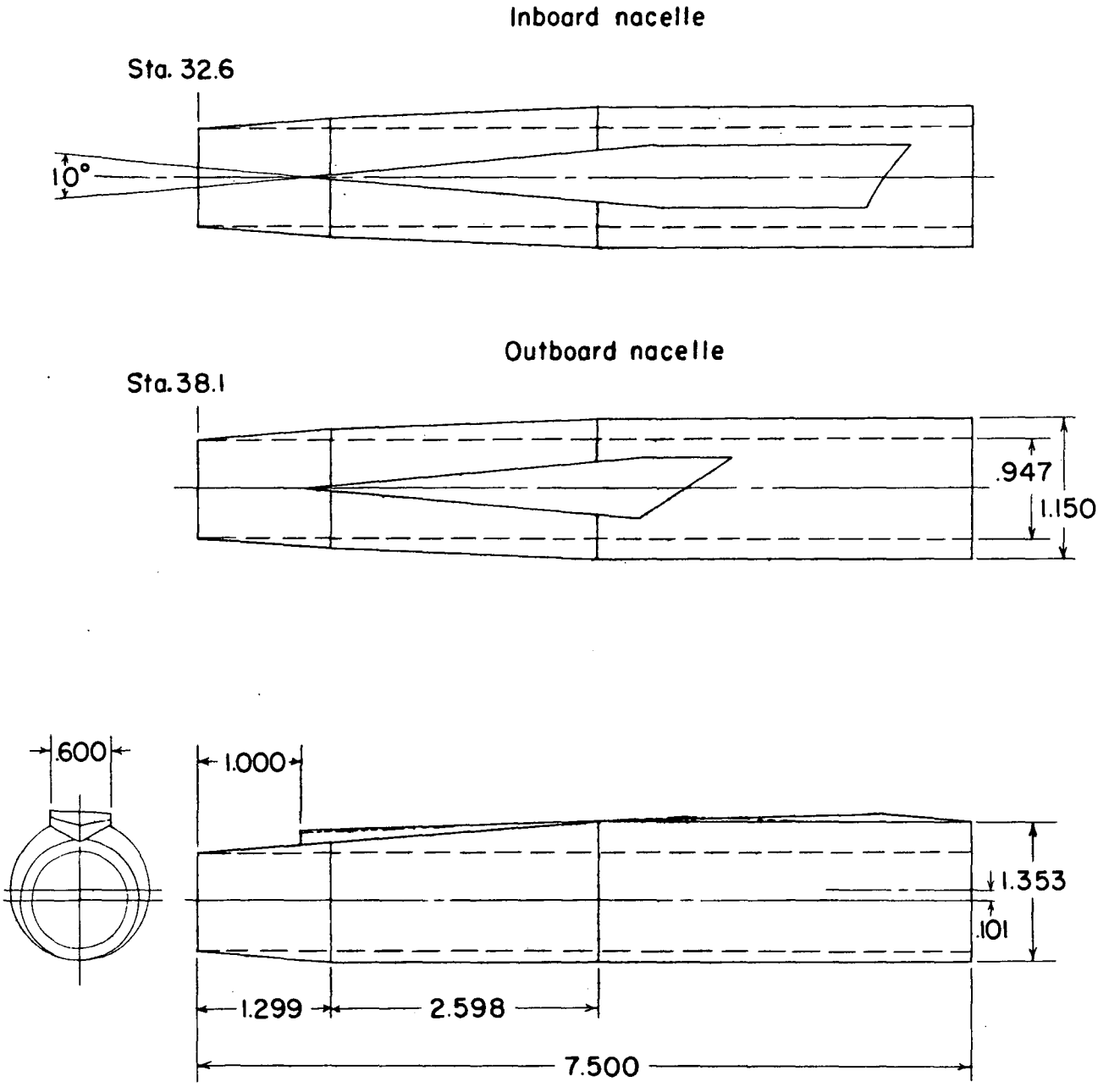


(d) Details of nacelles.

Figure 1.- Continued.

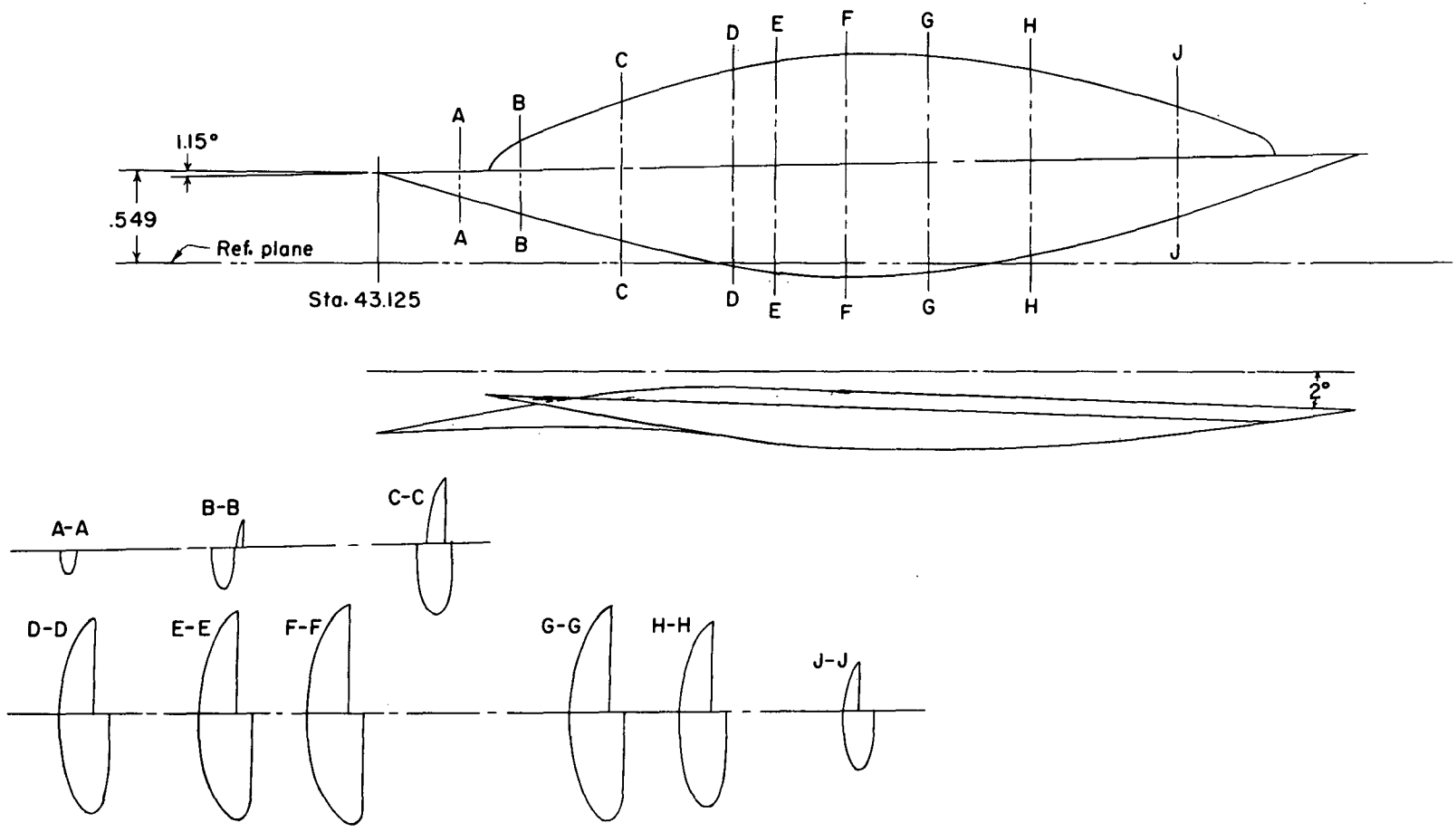


(e) Details of tail-mounting fairing.

Figure 1.- Concluded.

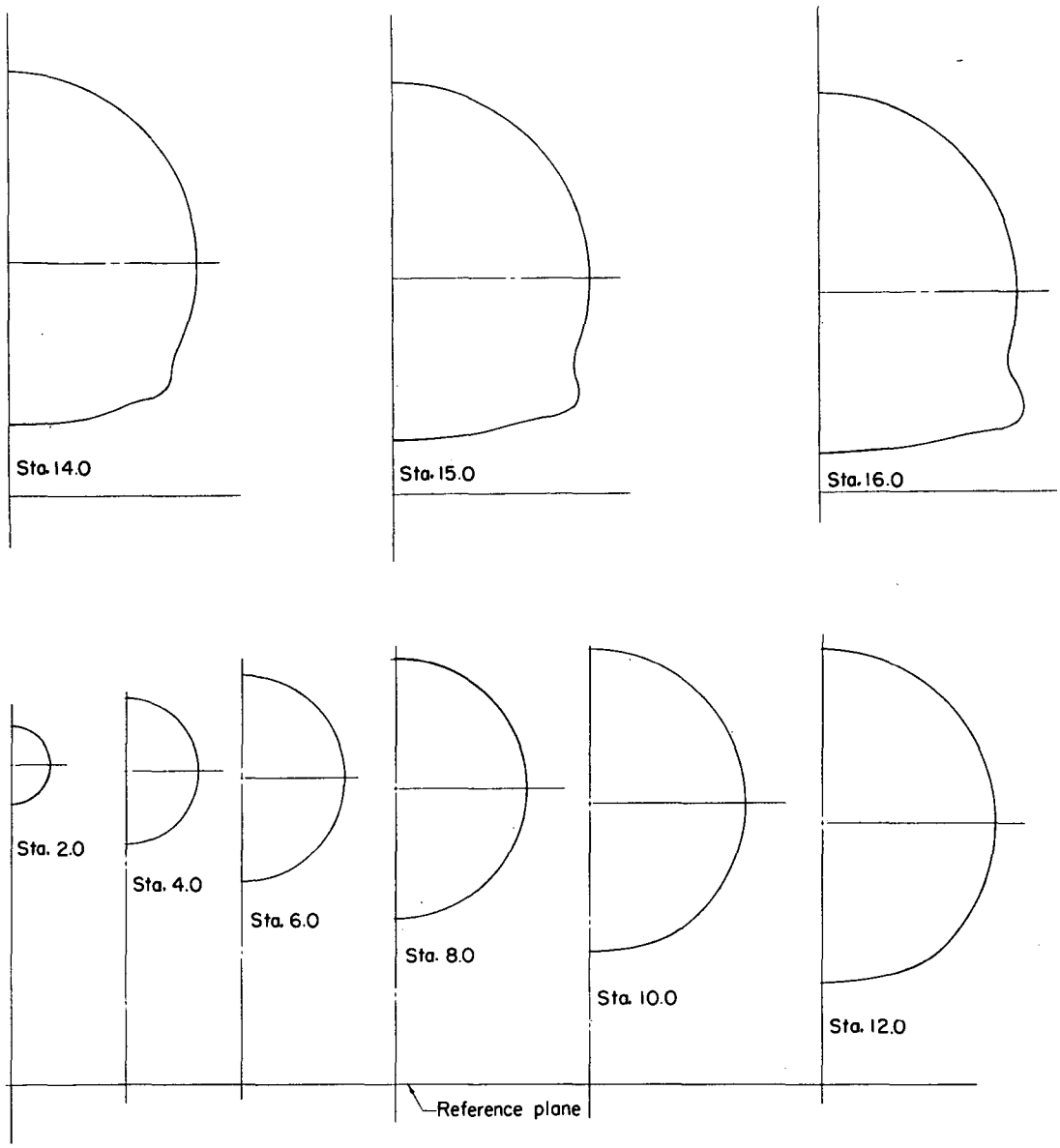


Figure 2.- Cross sections of various longitudinal stations.

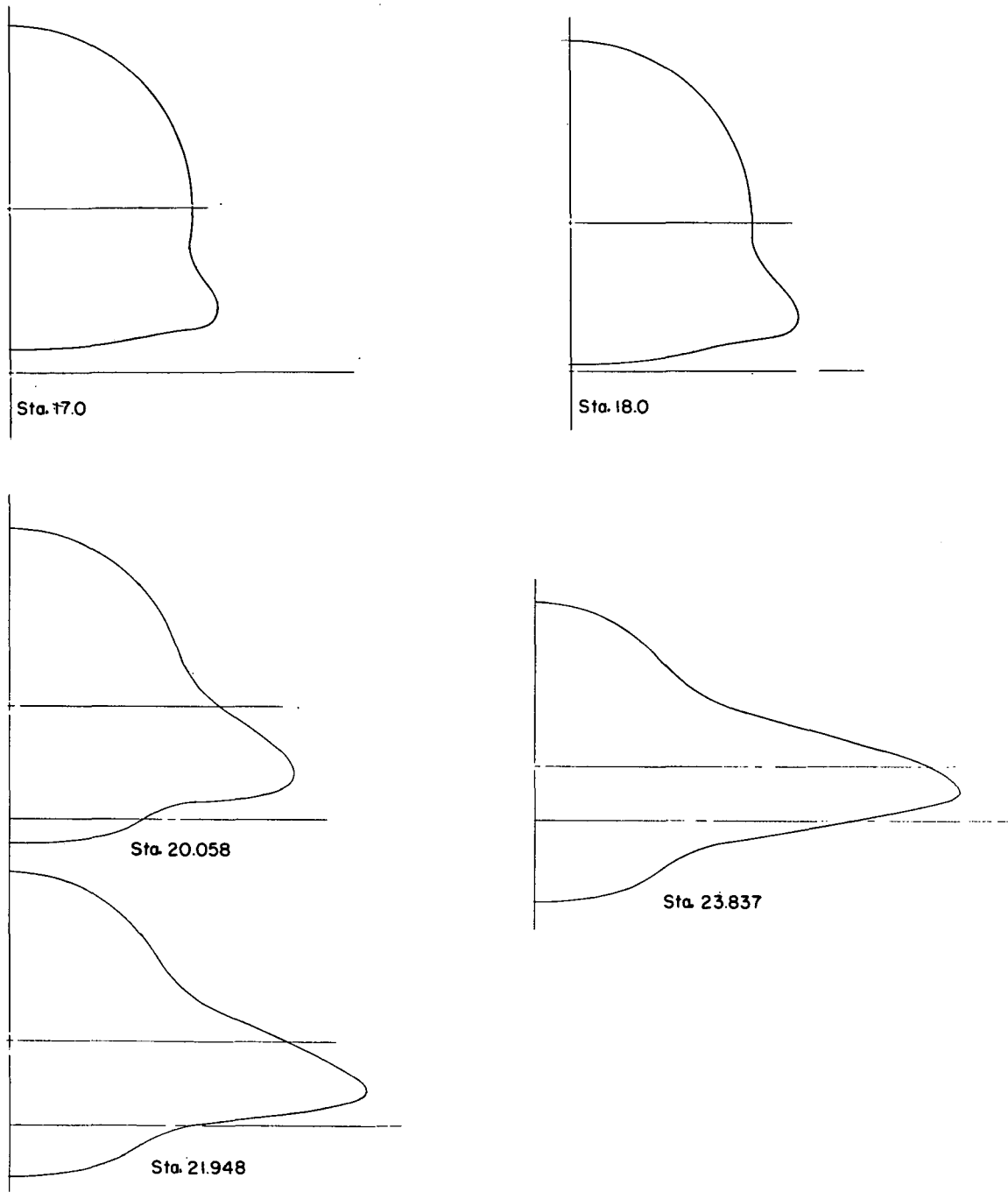


Figure 2.- Continued.

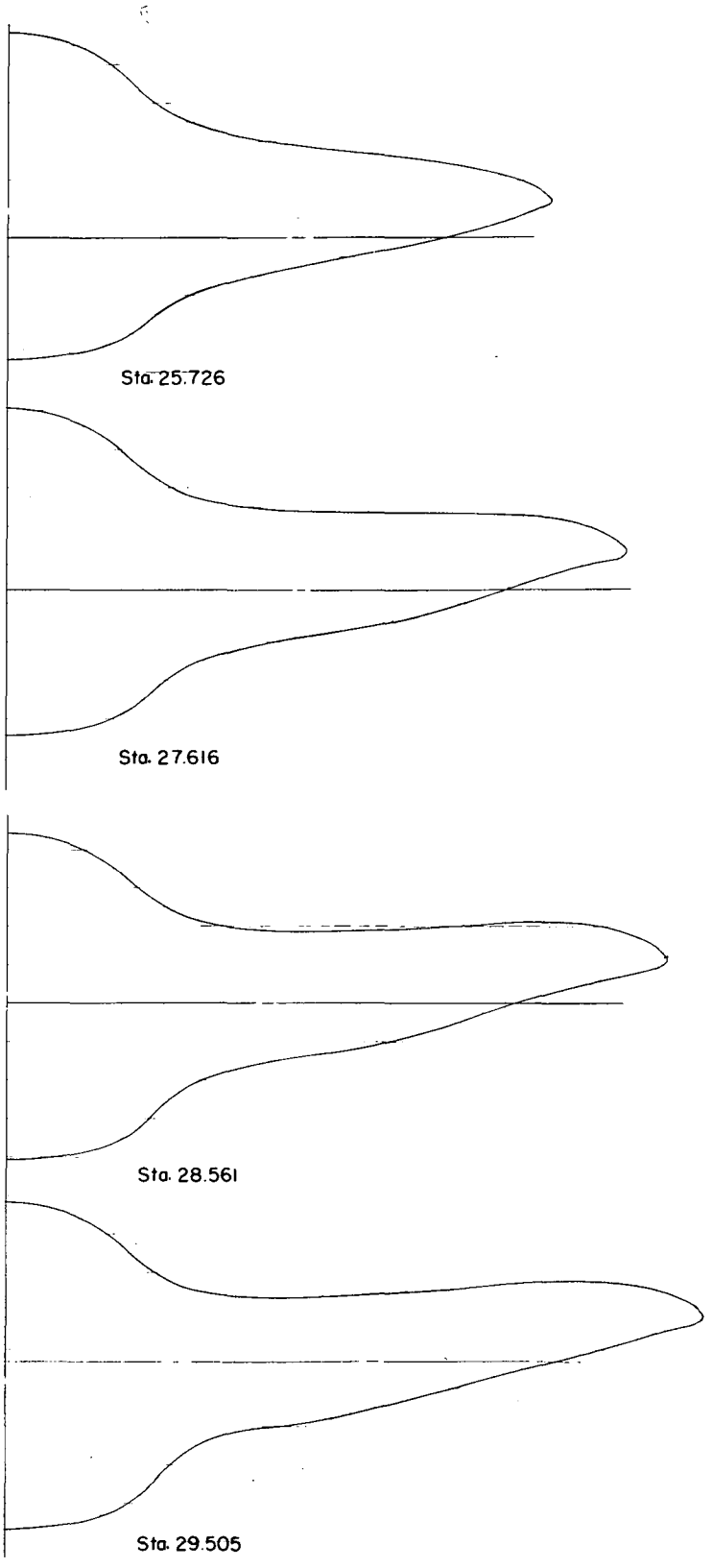


Figure 2.- Continued.

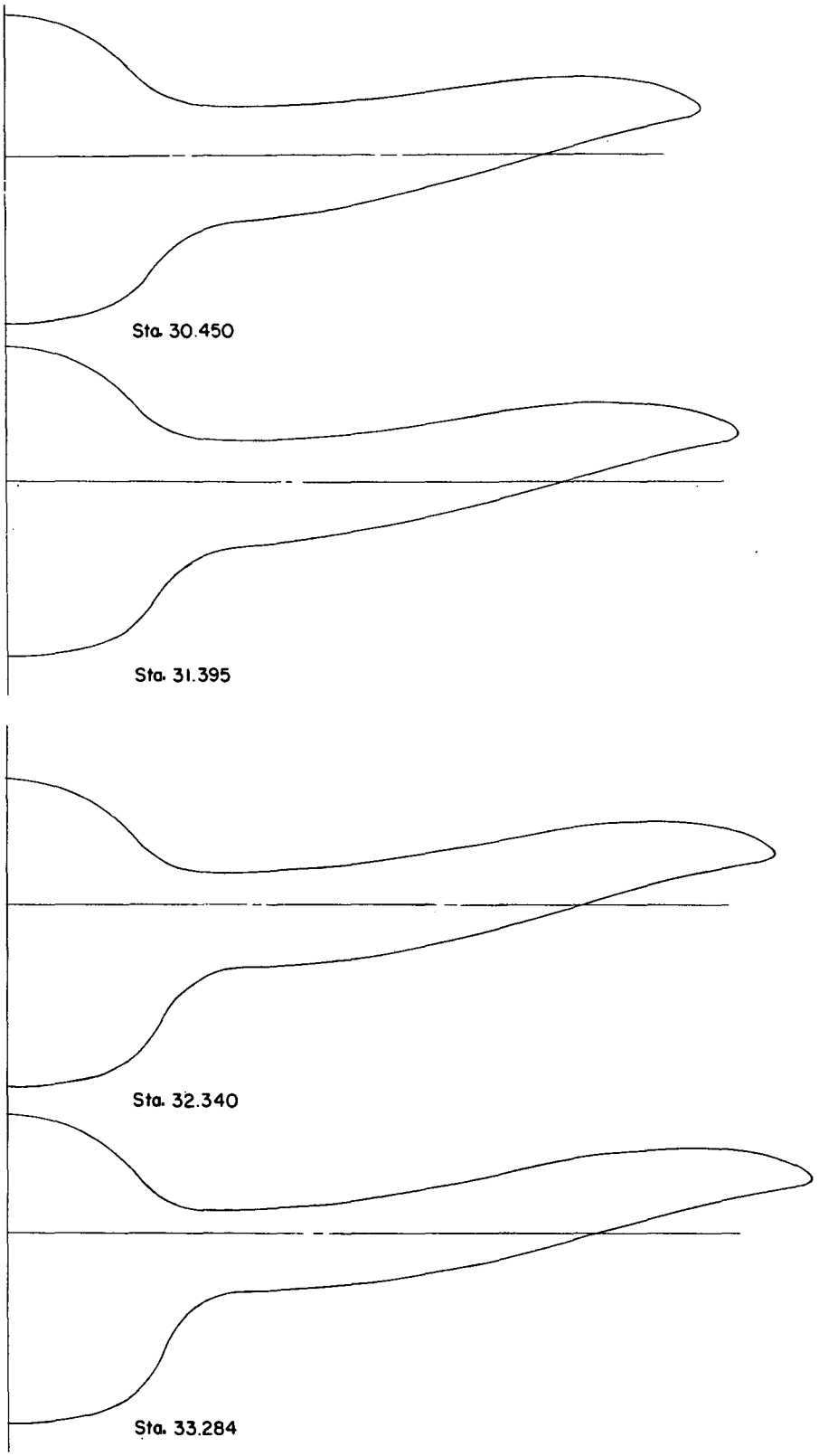


Figure 2.- Continued.

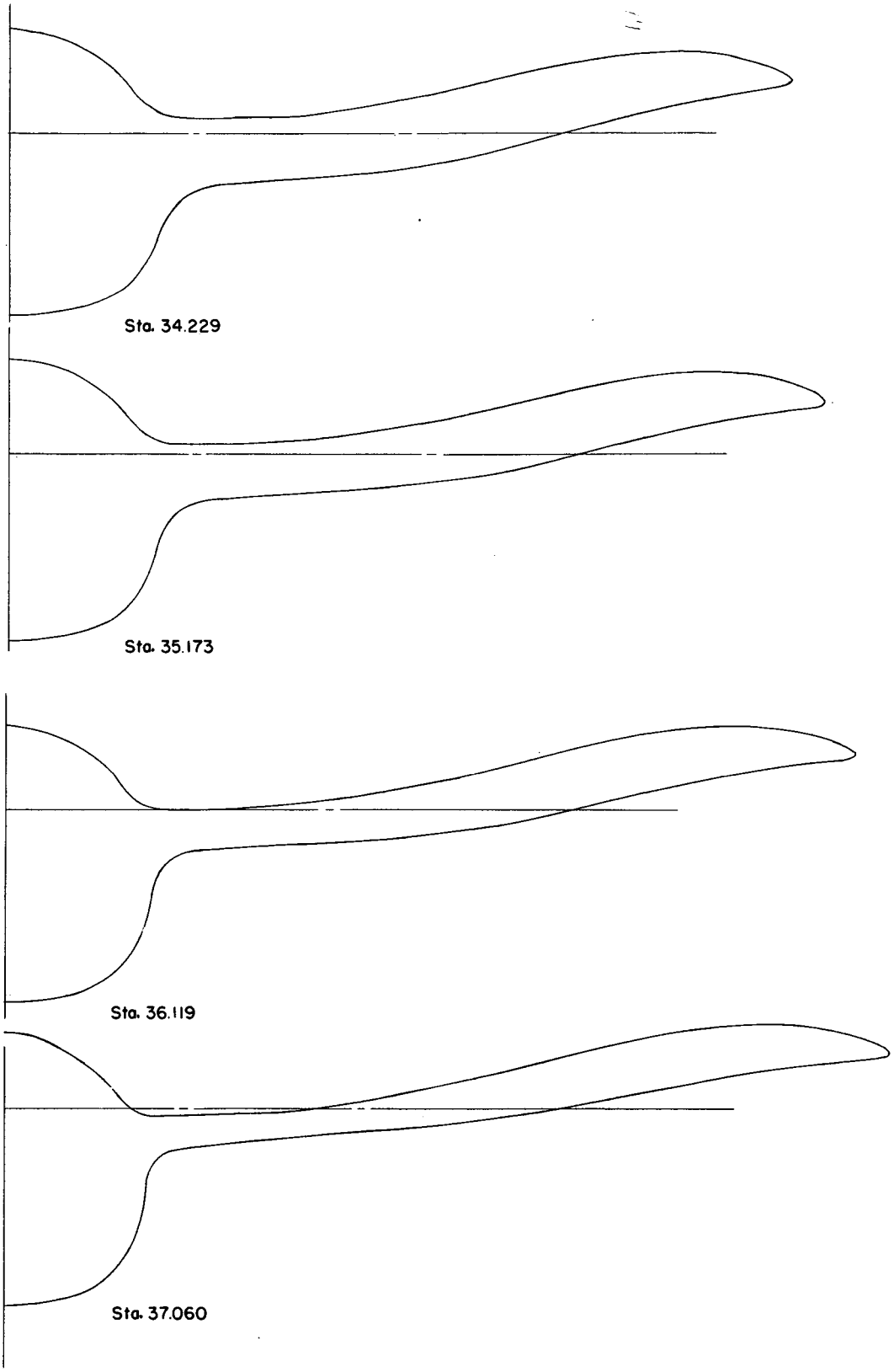


Figure 2.- Continued.

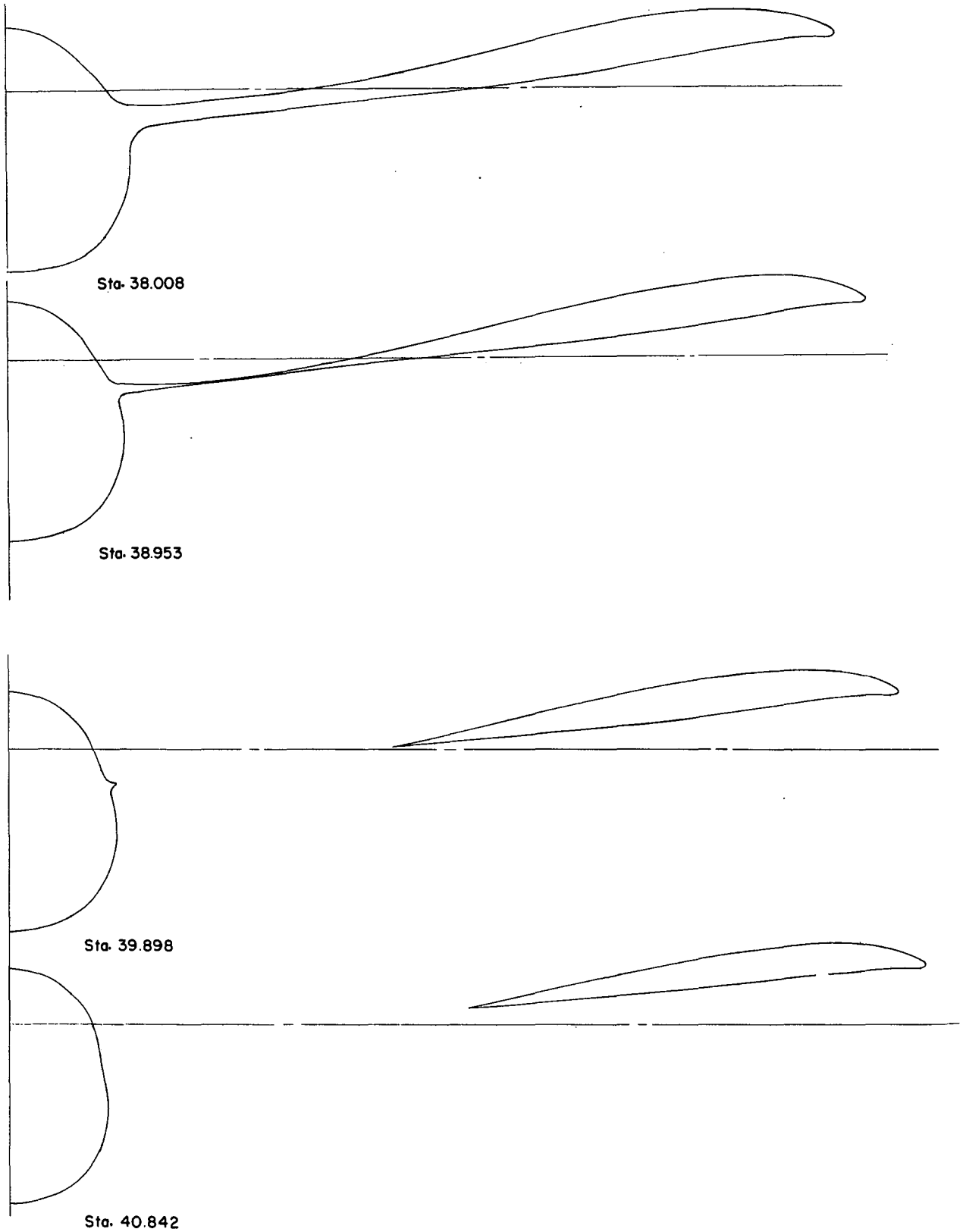


Figure 2.- Continued.

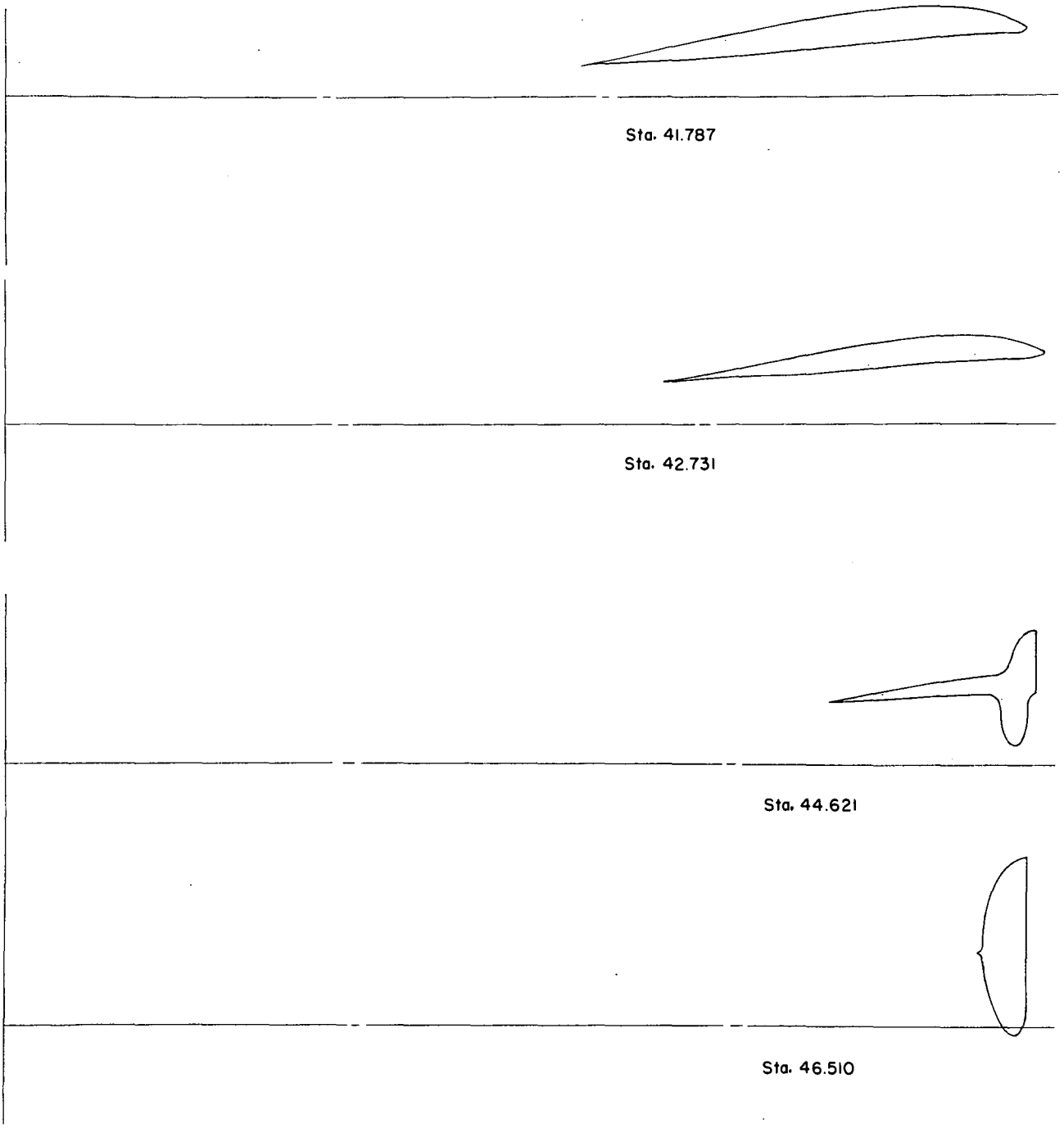


Figure 2.- Concluded.

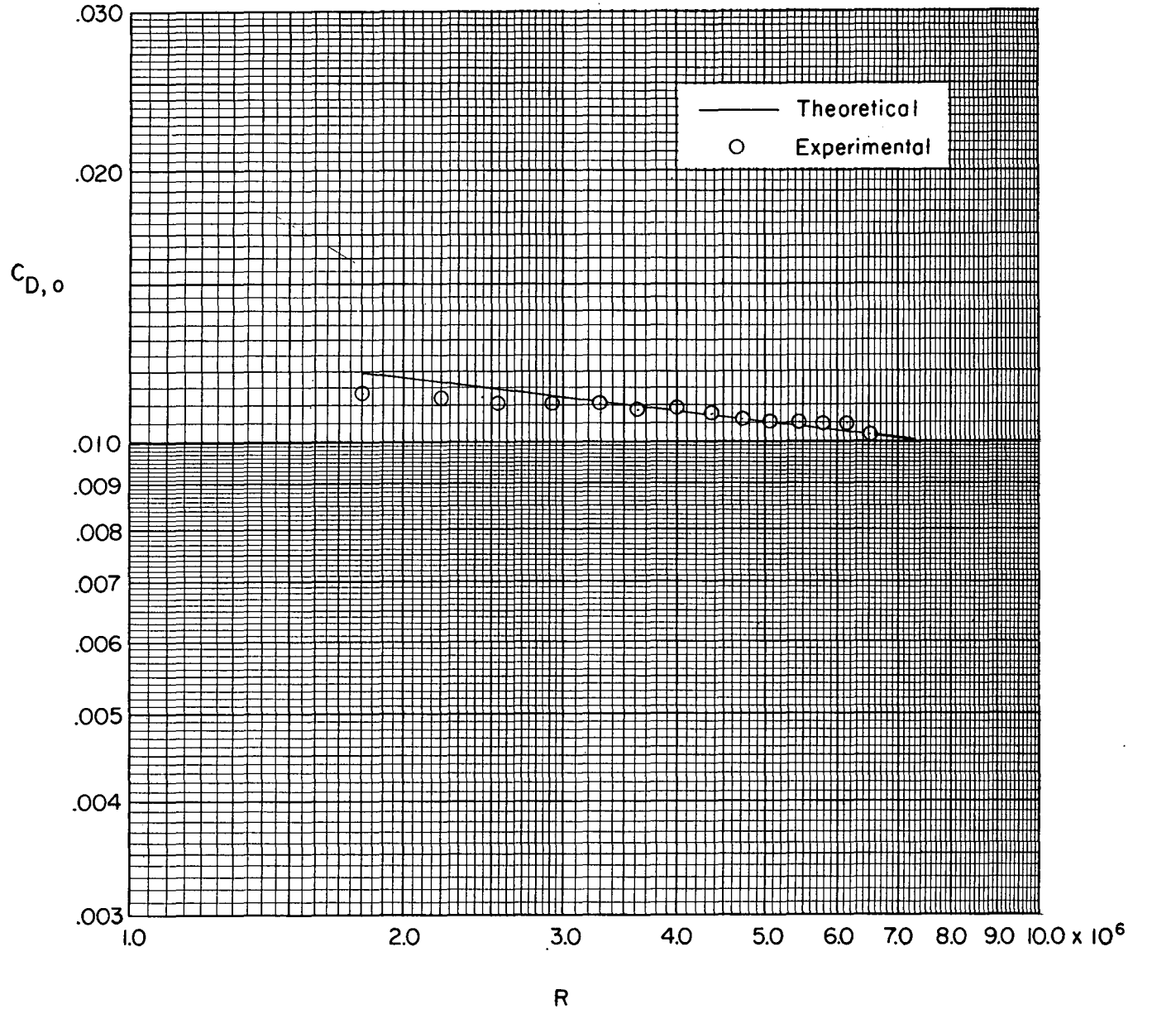


Figure 3.- Variation of zero-lift drag coefficient with Reynolds number for the complete configuration. M = 2.96; $\delta_h = -2^\circ$.

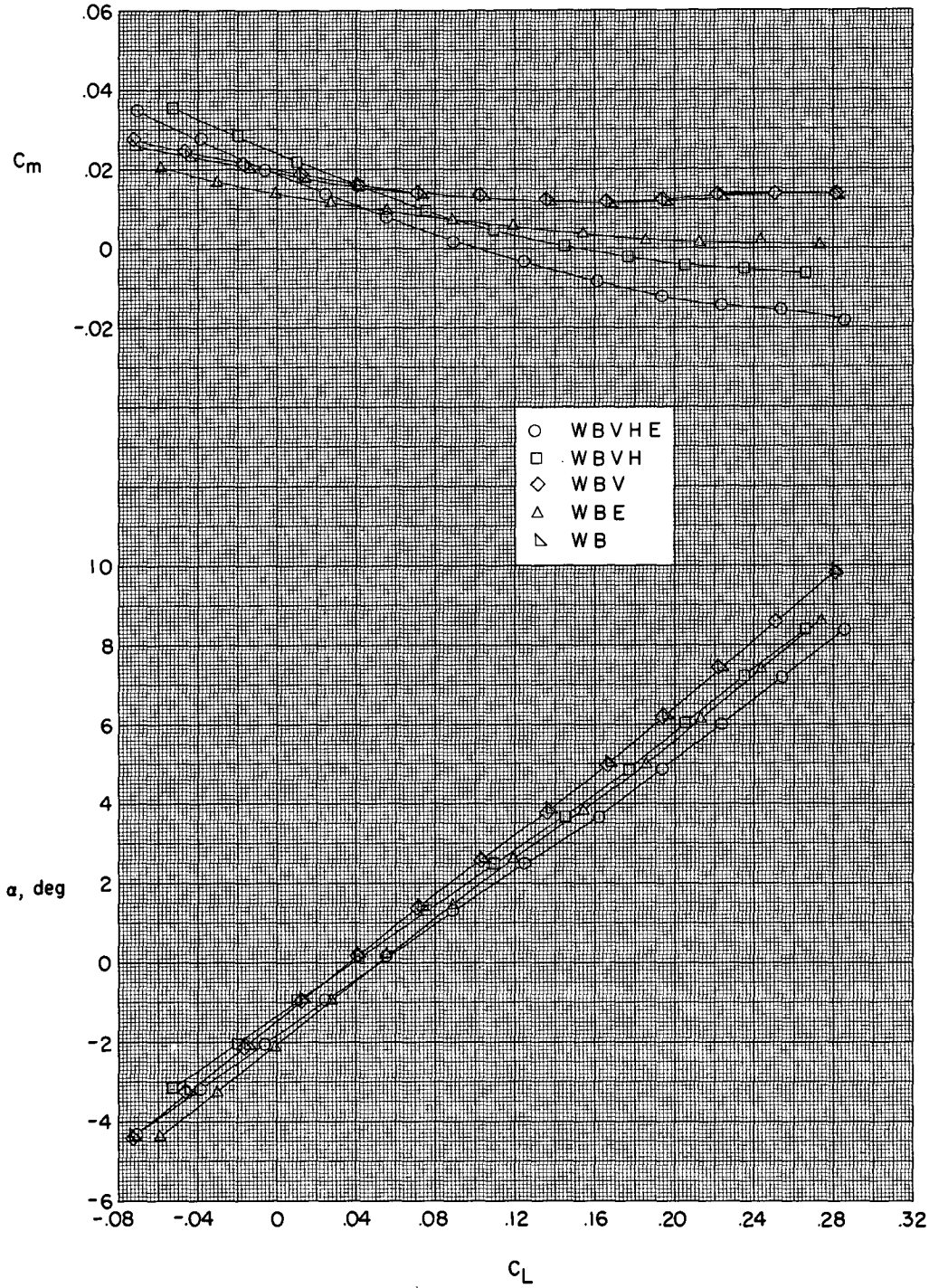


(a) M = 2.30.

Figure 4.- Effect of component parts on the aerodynamic characteristics in pitch.

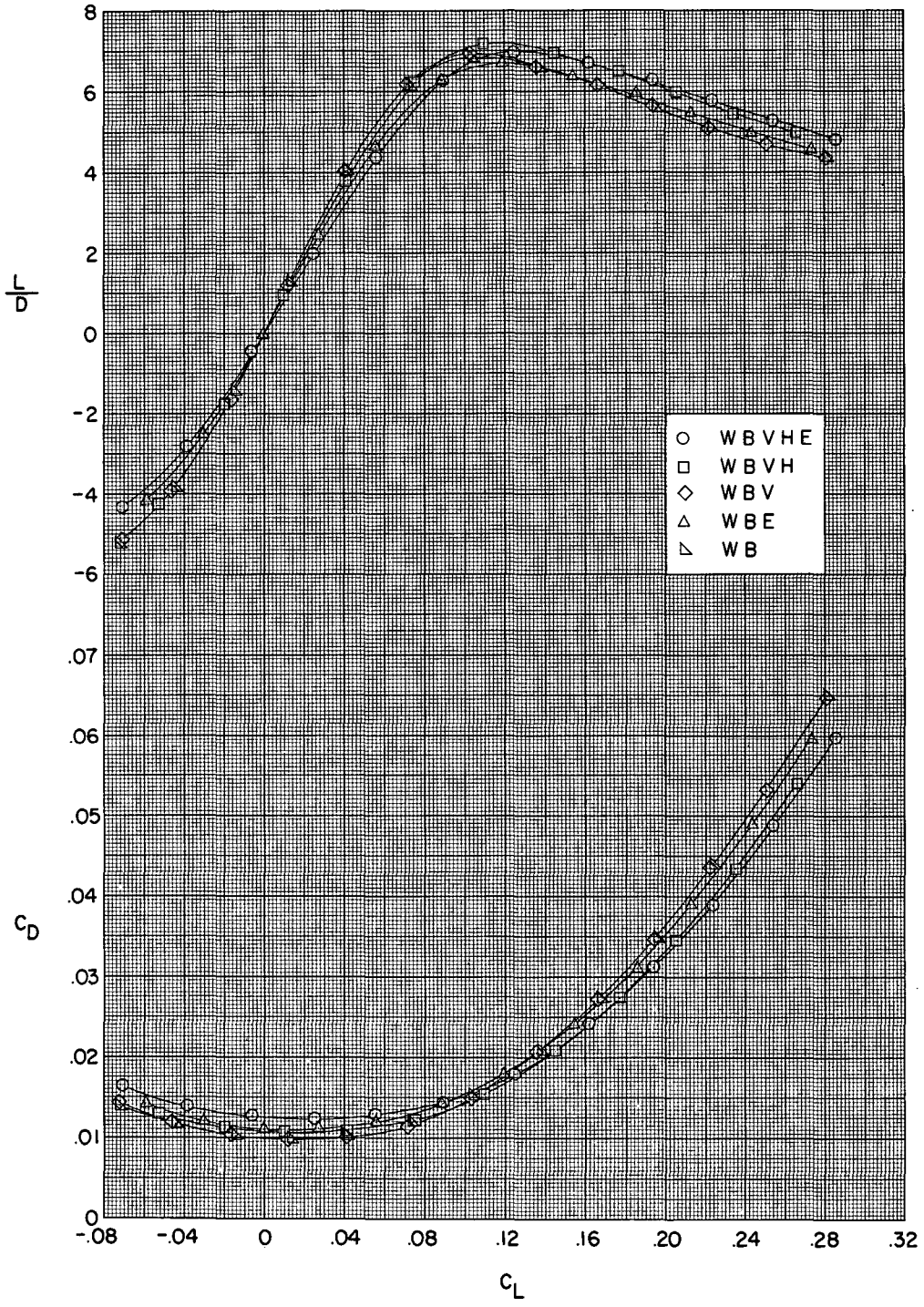


(a) Concluded.

Figure 4.- Continued.

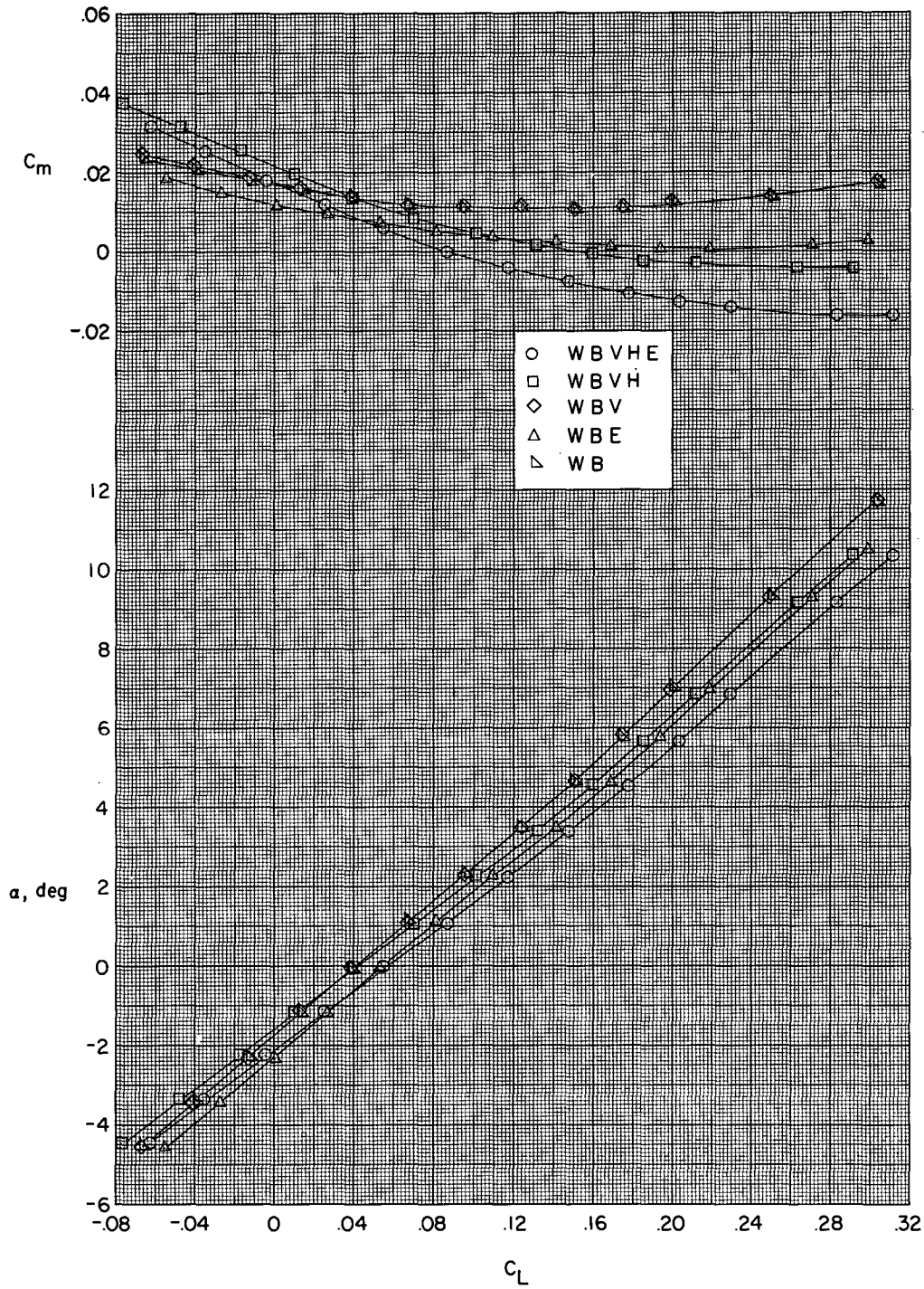


(b) M = 2.60.

Figure 4.- Continued.

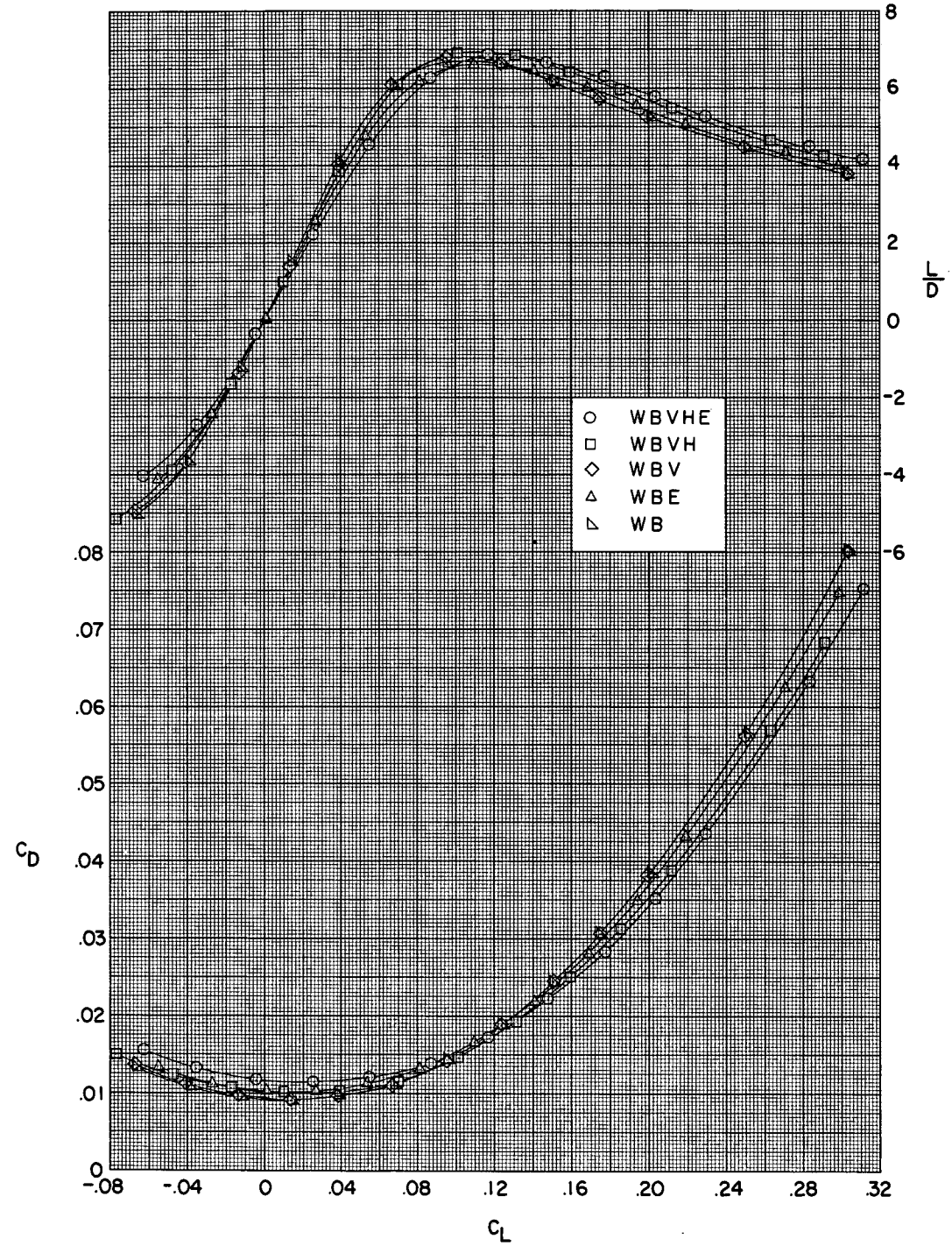


(b) Concluded.

Figure 4.- Continued.

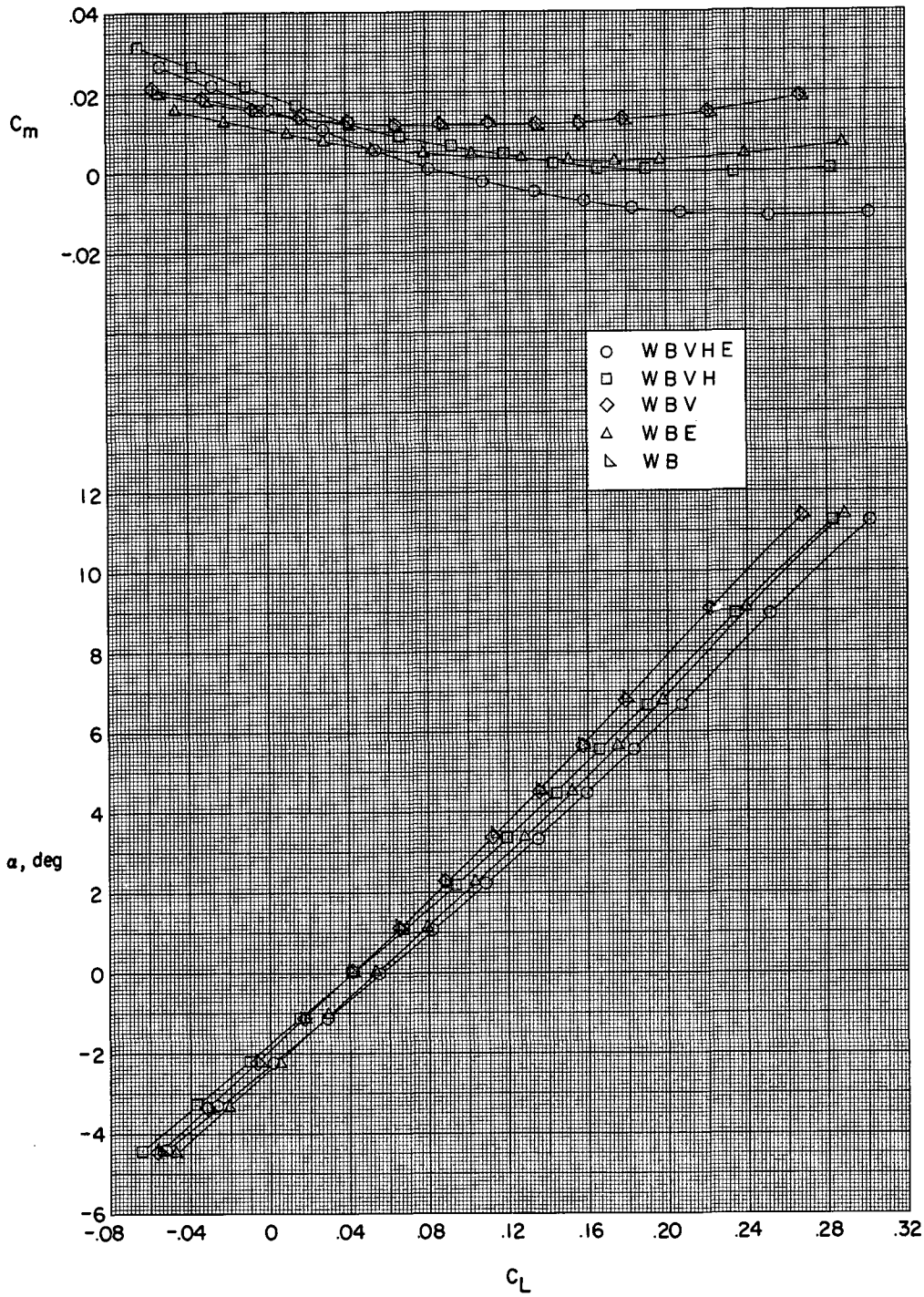


(c) M = 2.96.

Figure 4.- Continued.

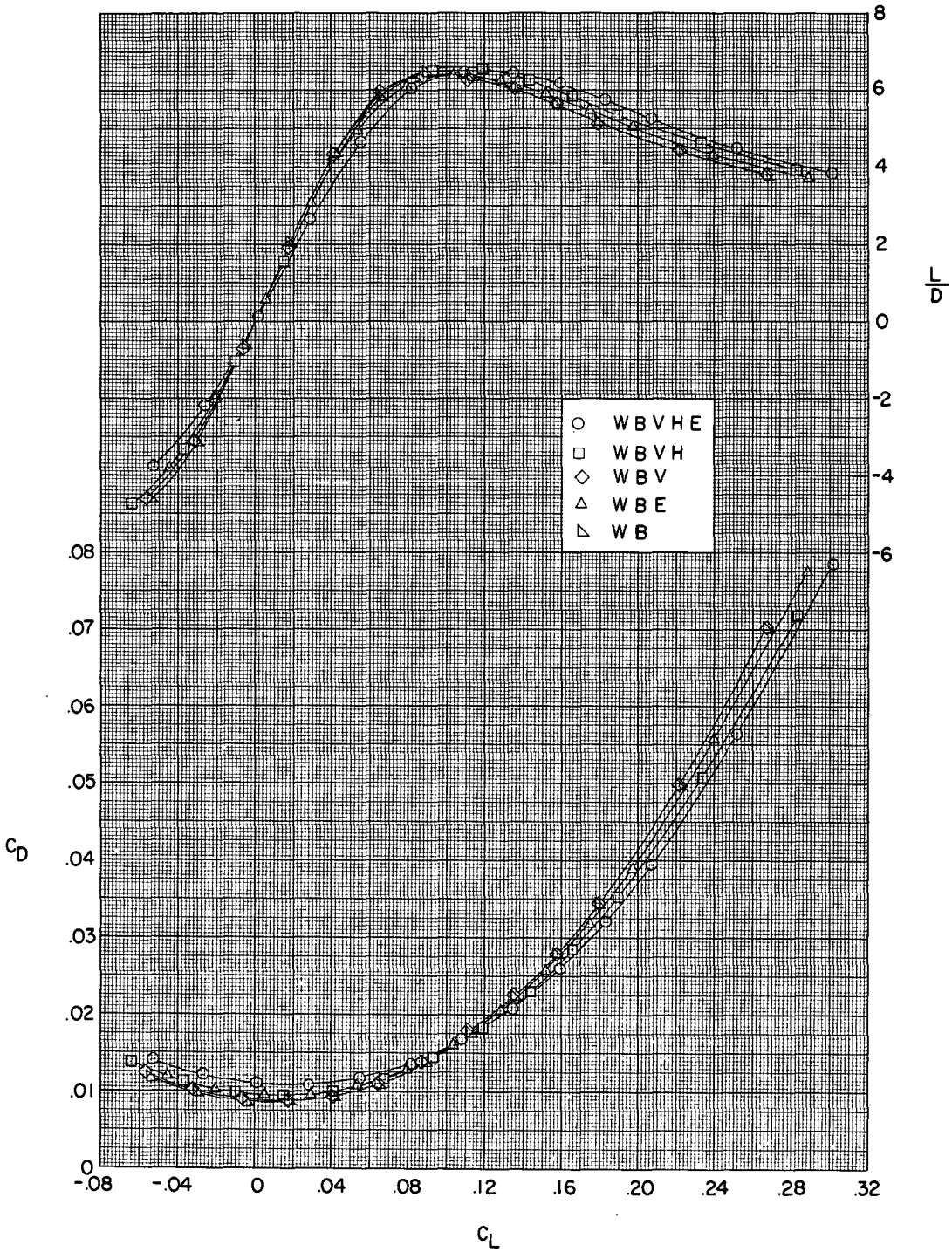


(c) Concluded.

Figure 4.- Concluded.

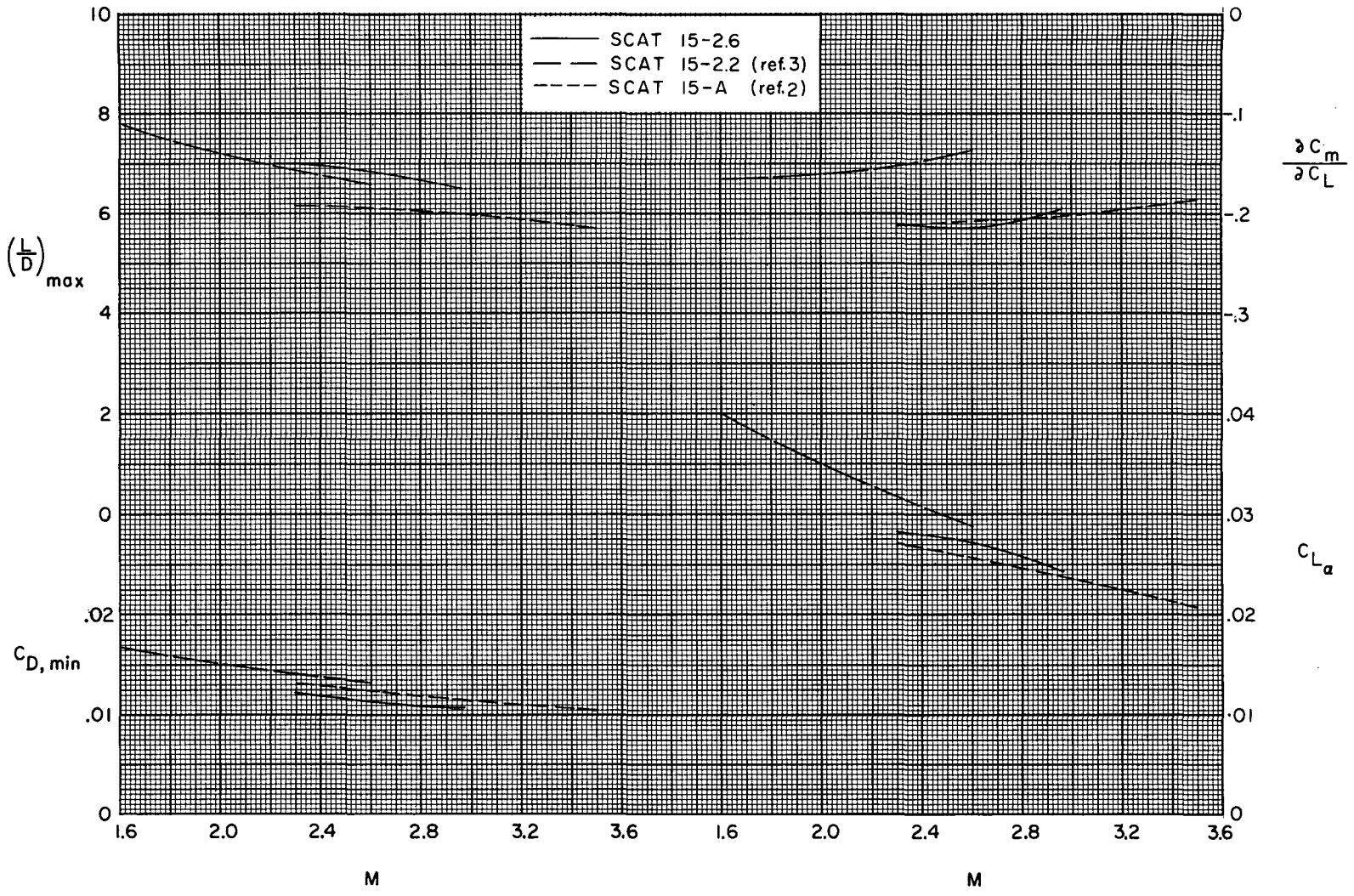


Figure 5.- Variation of longitudinal parameters with Mach number.

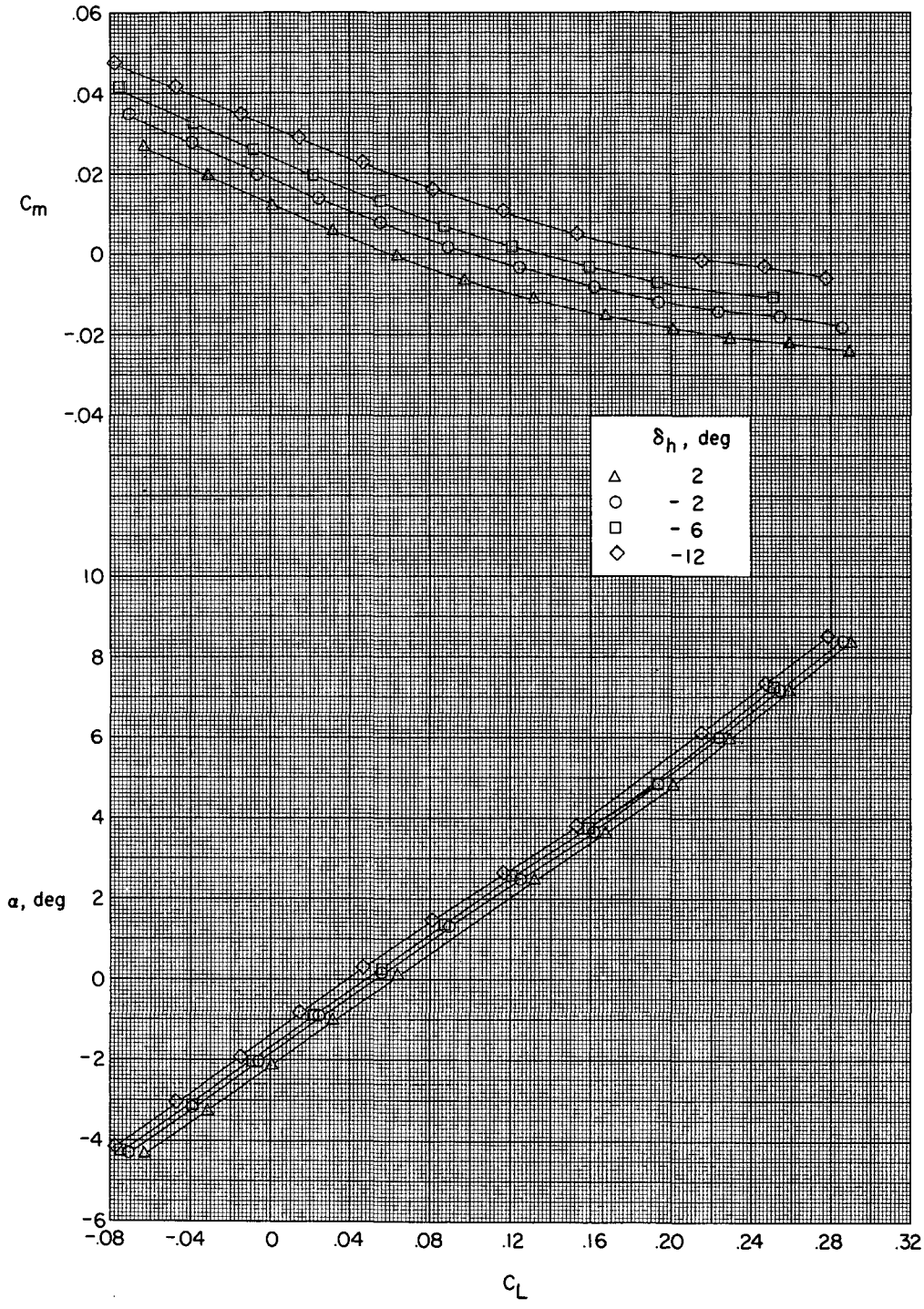


(a) M = 2.30.

Figure 6.- Effect of horizontal-tail deflection on the aerodynamic characteristics in pitch.

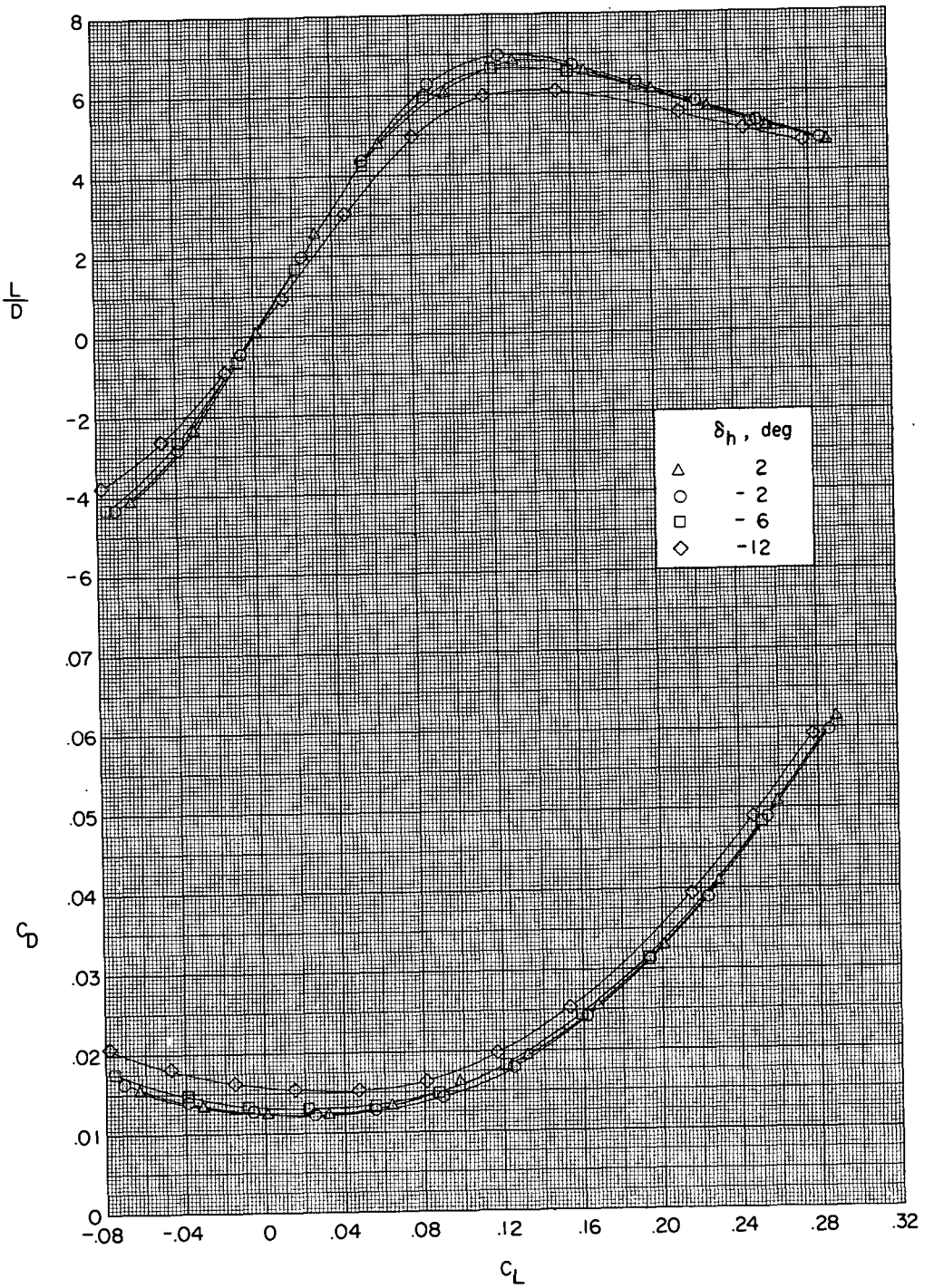


(a) Concluded.

Figure 6.- Continued.

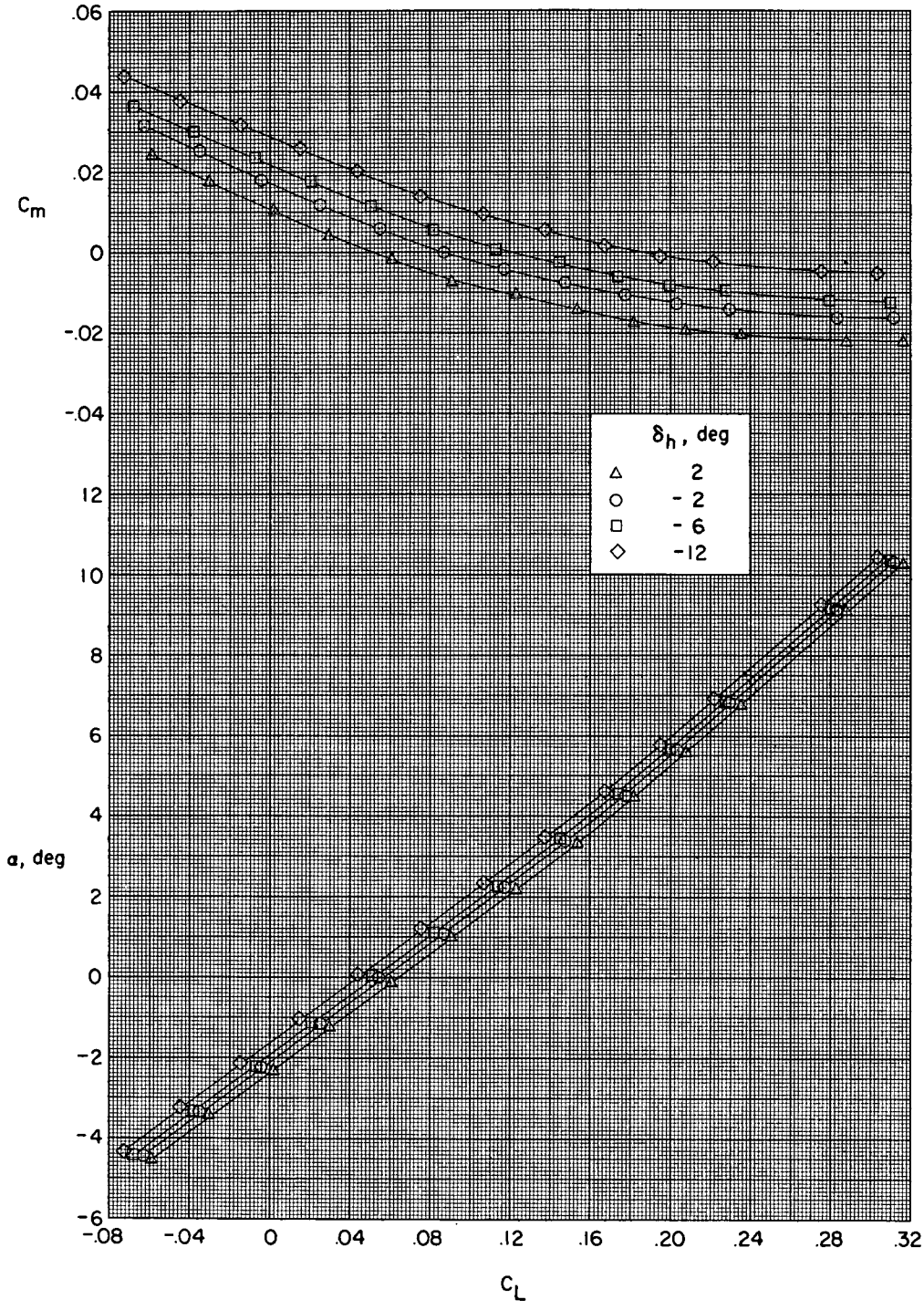


(b) M = 2.60.

Figure 6.- Continued.

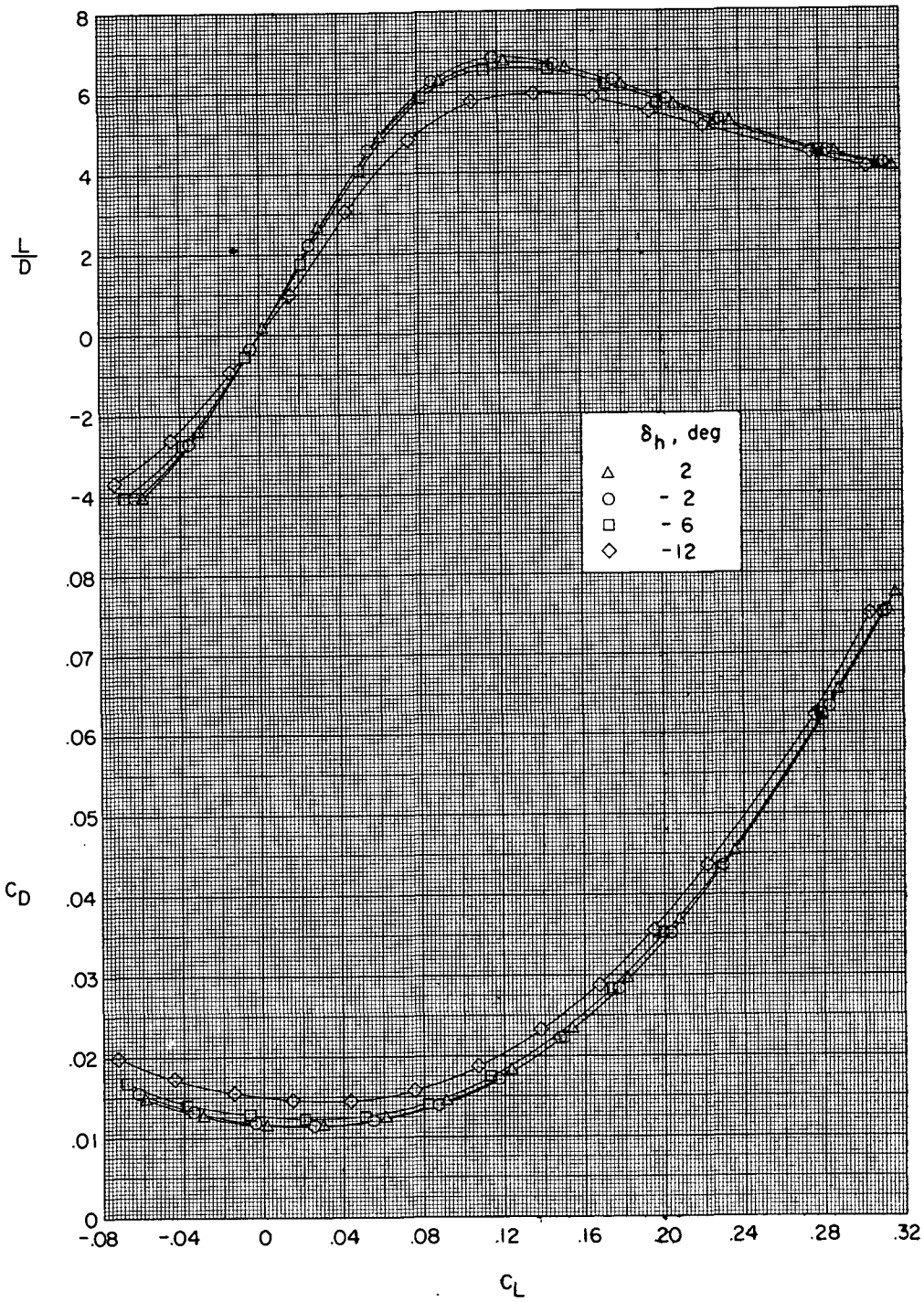


(b) Concluded.

Figure 6.- Continued.

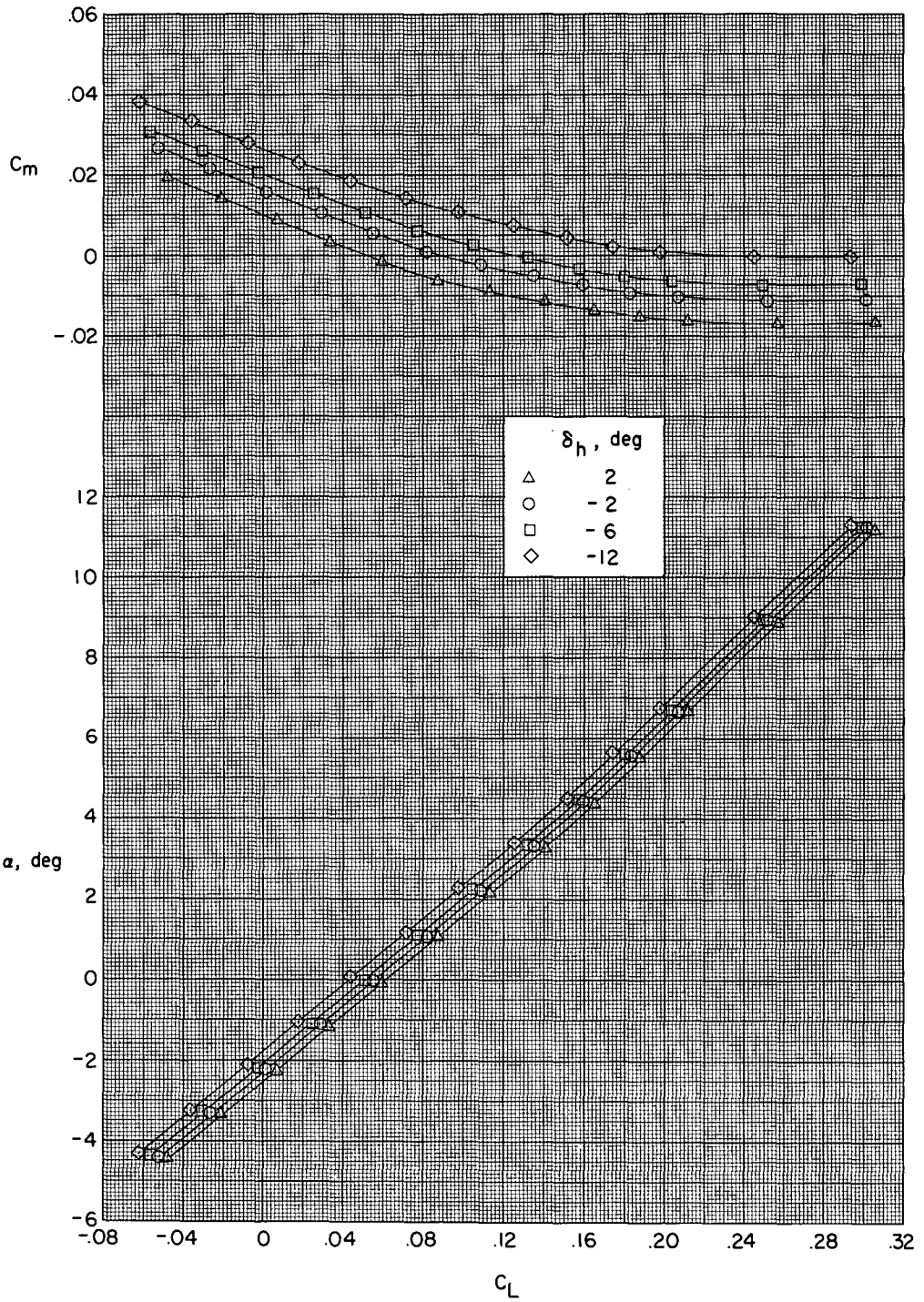


(c) M = 2.96.

Figure 6.- Continued.

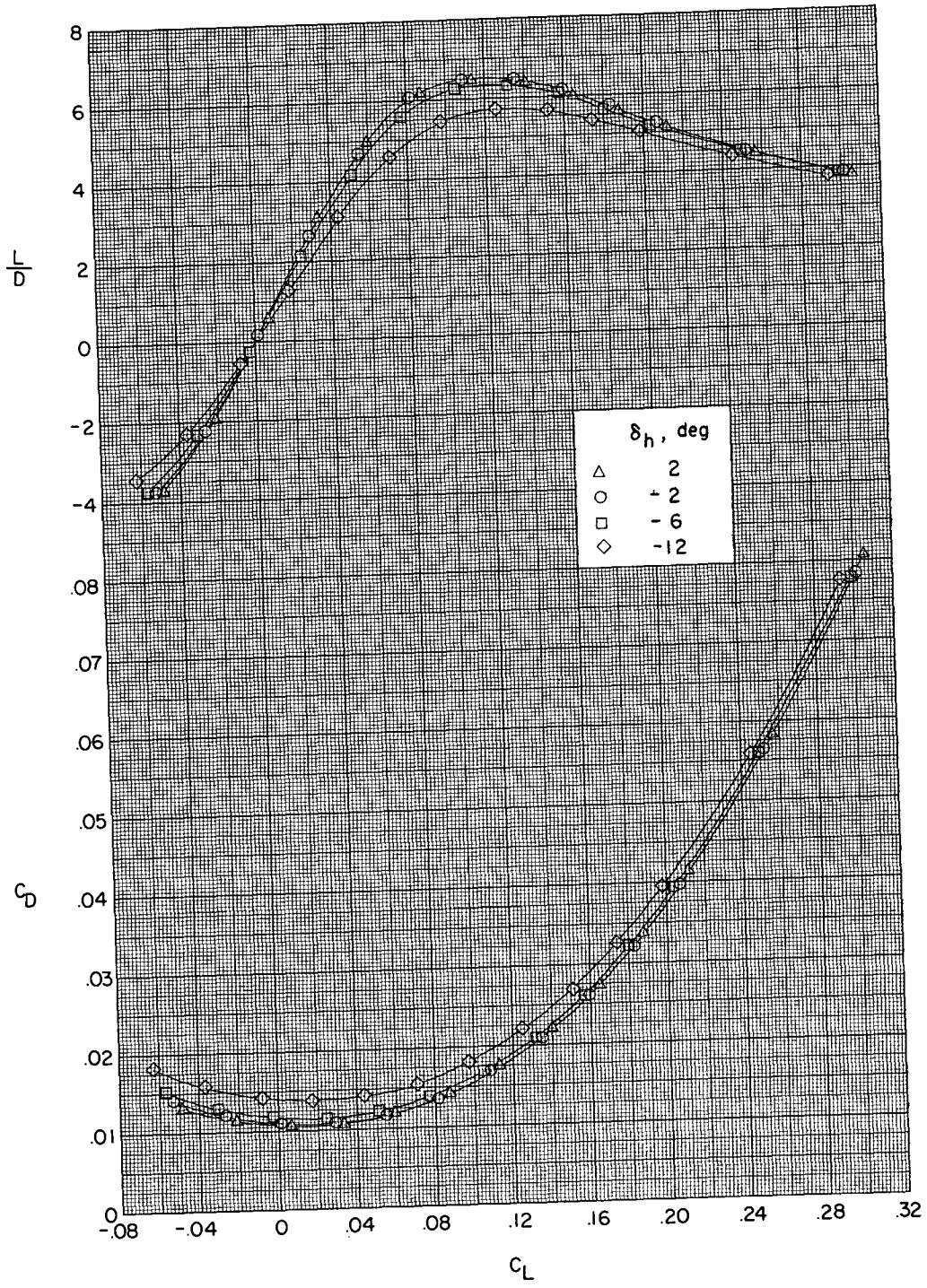


(c) Concluded.

Figure 6.- Concluded.

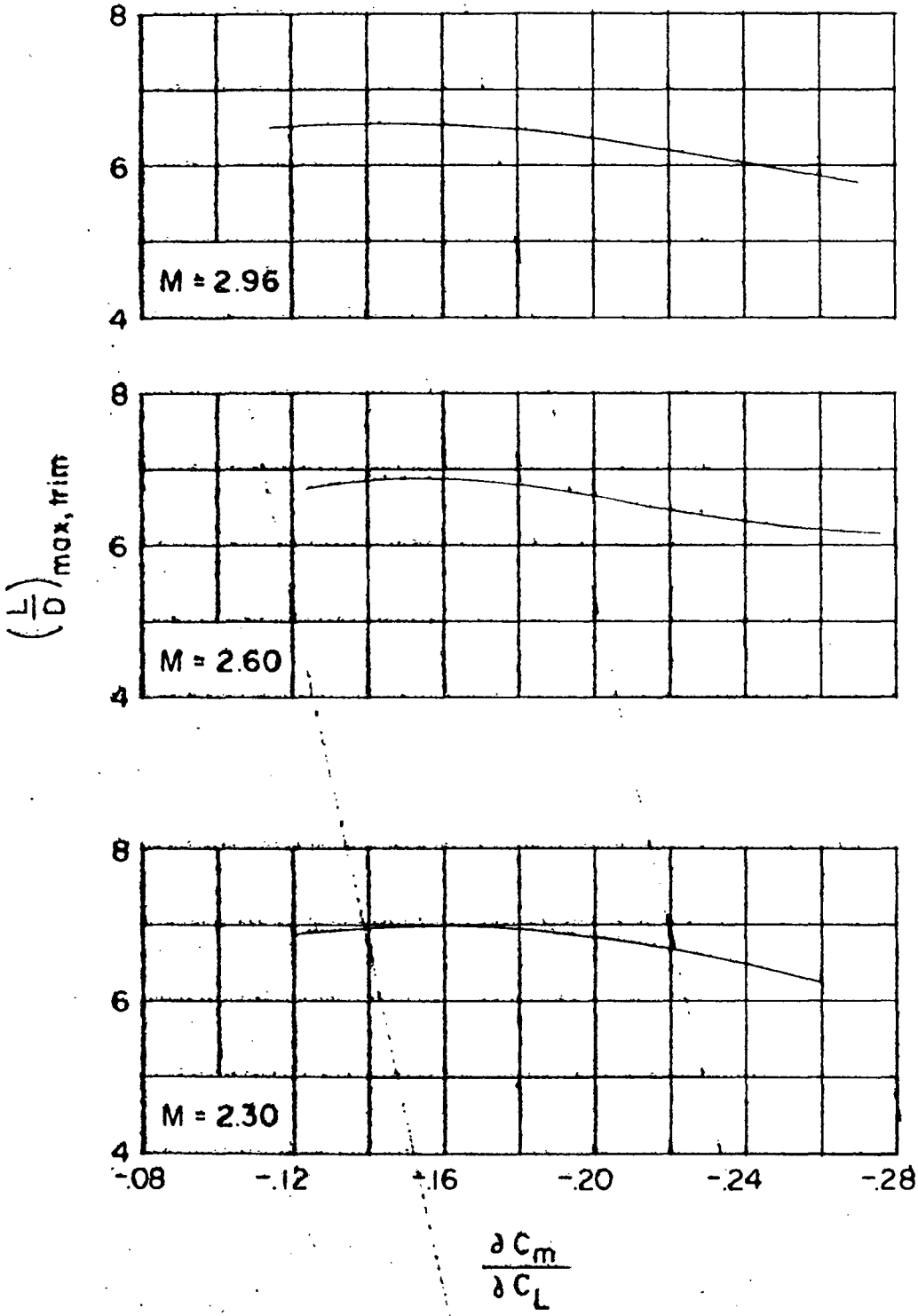


Figure 7.- Variation of maximum trimmed L/D with $\frac{\partial C_m}{\partial C_L}$.

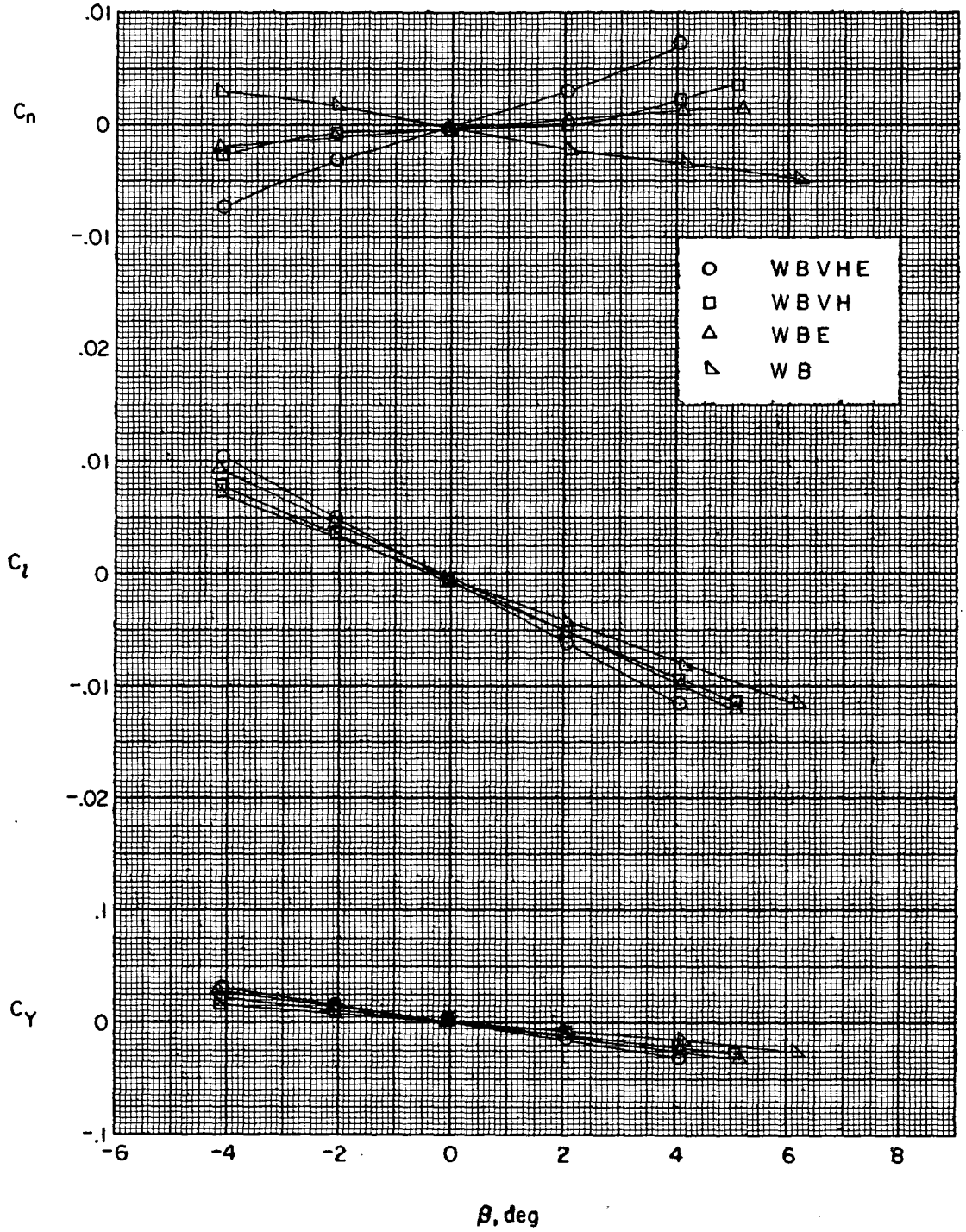


(a) $M = 2.30$; $\alpha \approx 3.7°$.

Figure 8.- Aerodynamic characteristics in sideslip for various configurations.

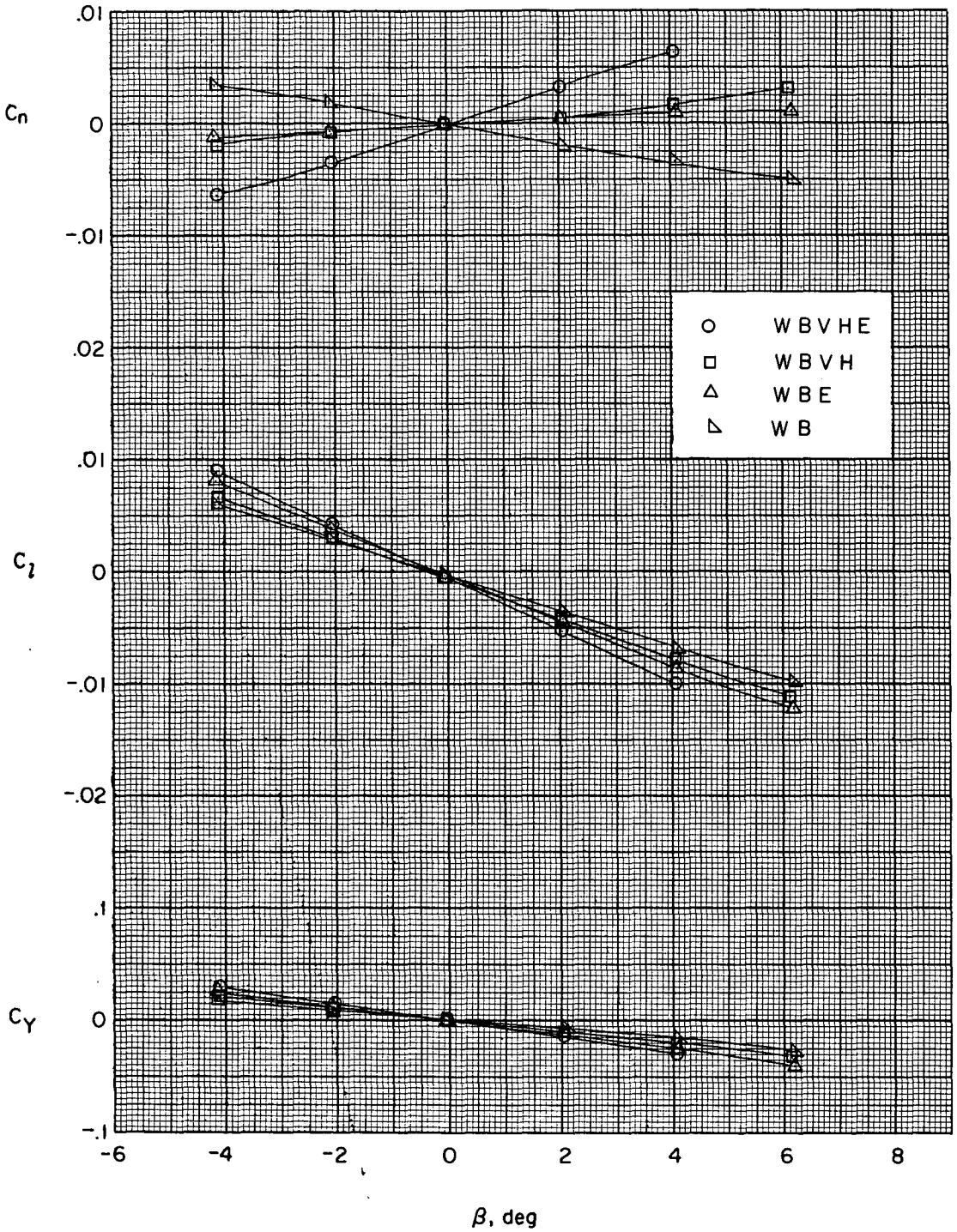


(b) M = 2.60; $\alpha \approx 3.4^{\circ}$.

Figure 8.- Continued.

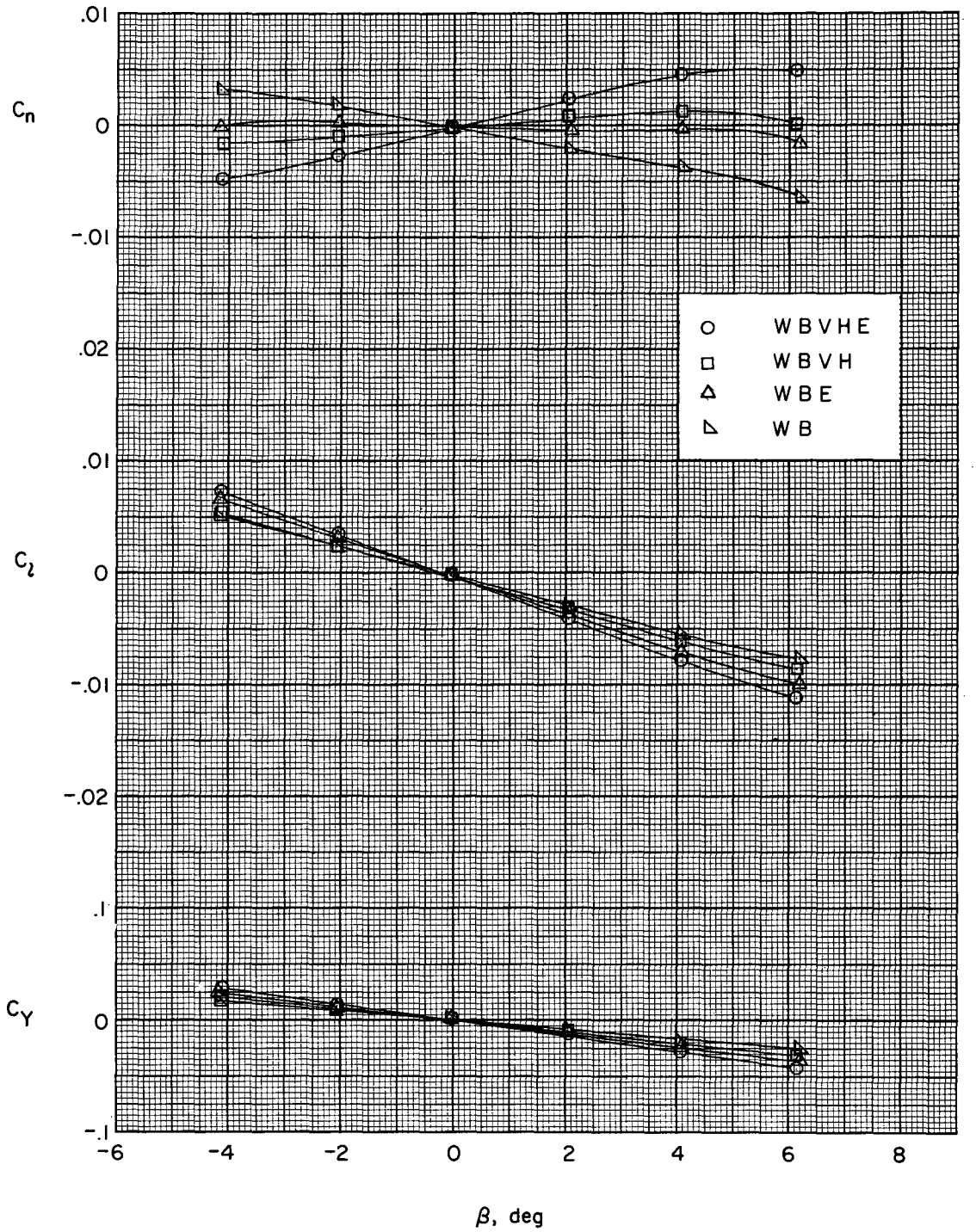


(c) M = 2.96; $\alpha \approx 3.3^\circ$.

Figure 8.- Concluded.

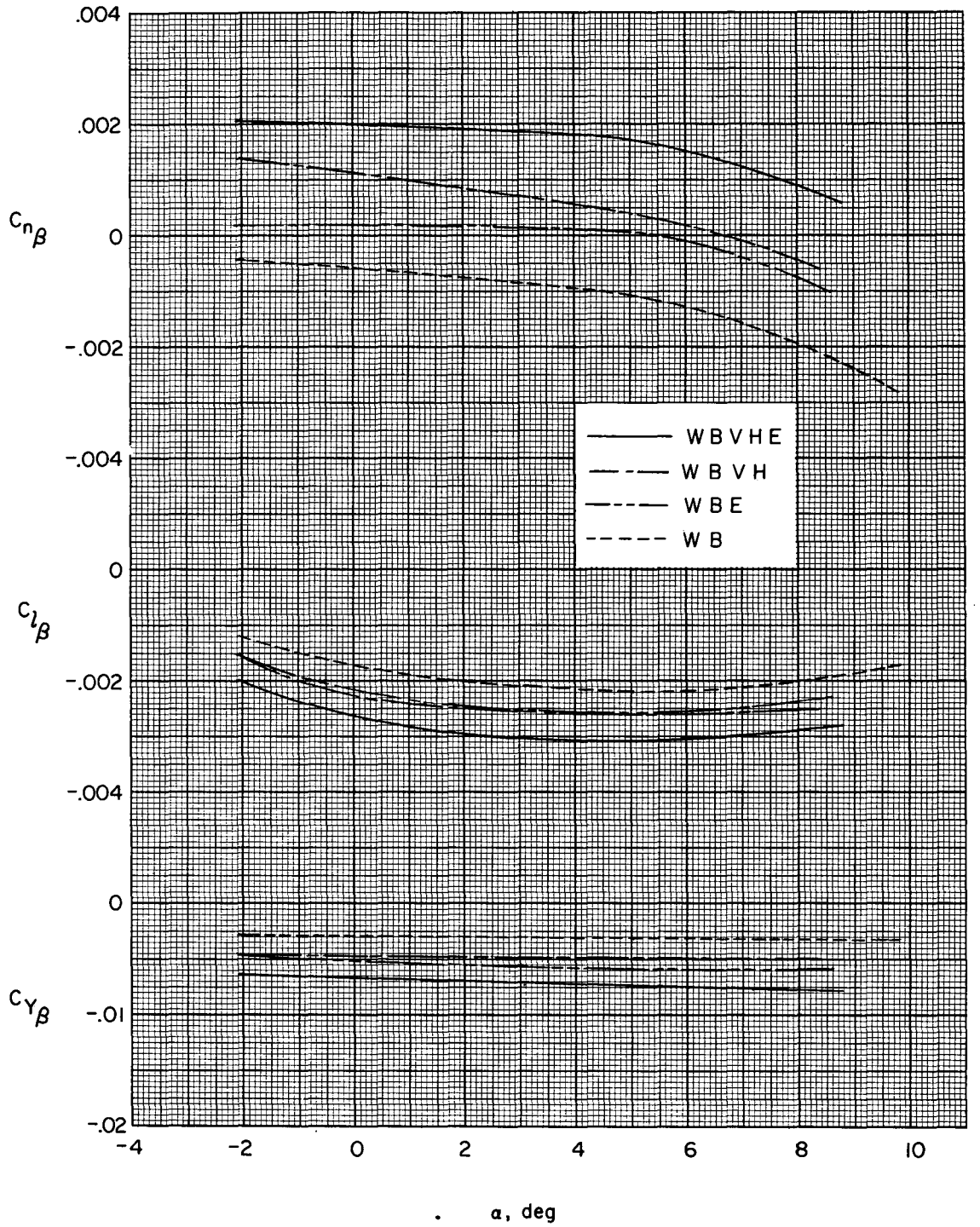


(a) M = 2.30.

Figure 9.- Variation of sideslip derivatives with angle of attack.

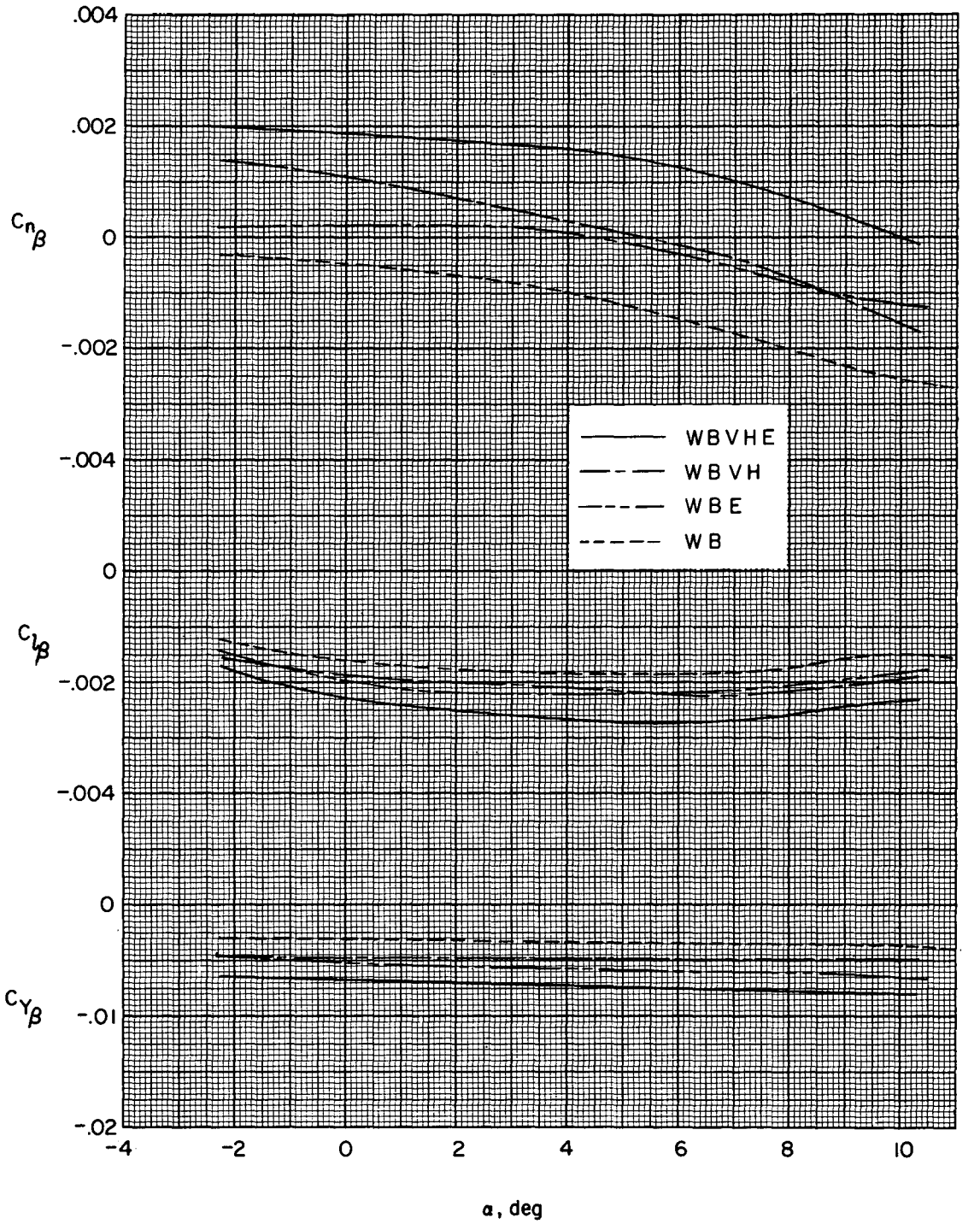


(b) M = 2.60.

Figure 9.- Continued.

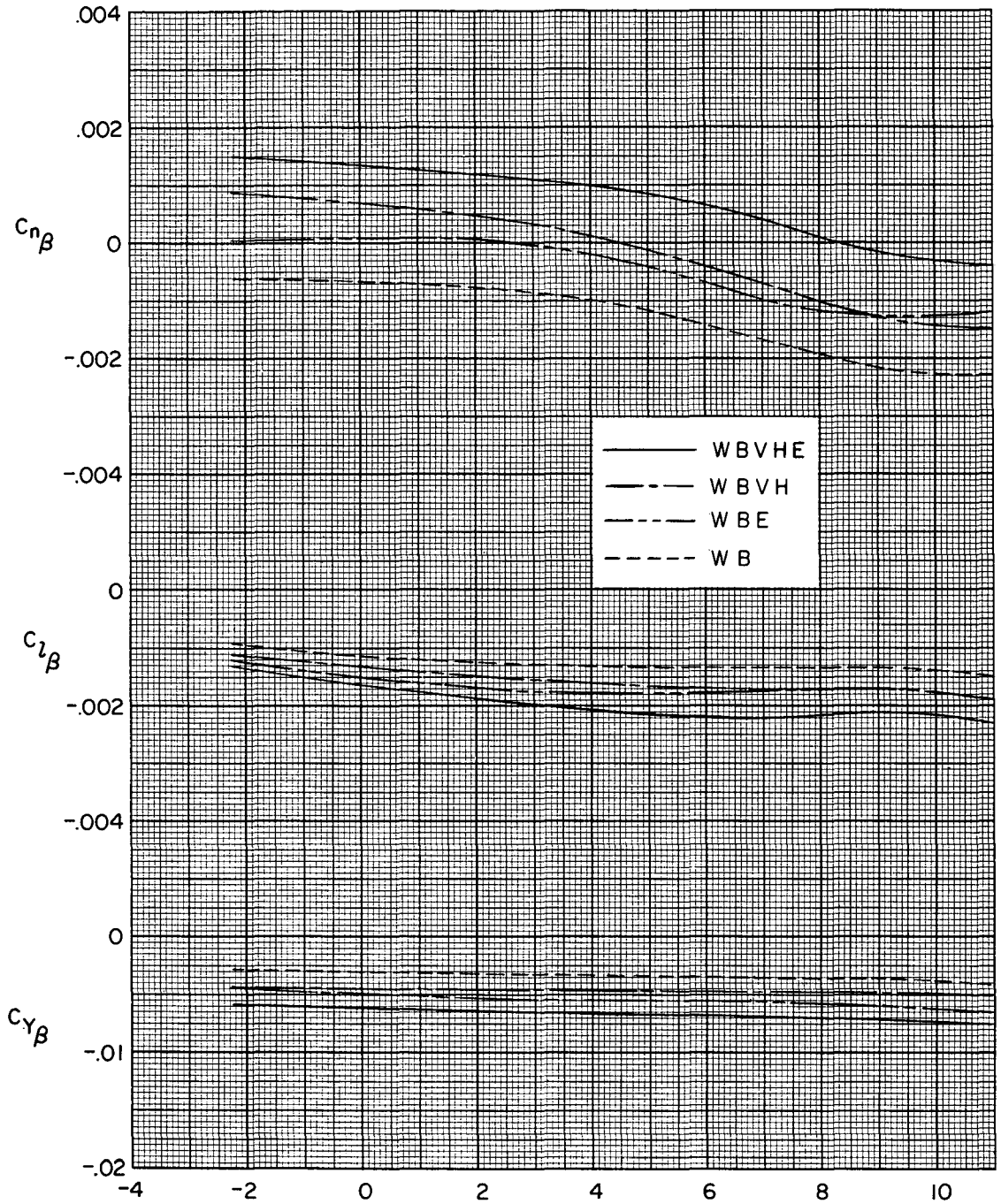


(c) M = 2.96.

Figure 9.- Concluded.



NASA-Langley, 1963 L-3402